Uncertainty, Social Valuation, and Climate Change Policy*

Michael Barnett* William Brock** Lars Peter Hansen‡
Hong Zhang‡‡

June 26, 2024

Abstract

Uncertainty, as it pertains to climate change and other policy challenges, operates through multiple channels. Such challenges are commonly framed using social valuations such as the social cost of climate change and the social value of research and development. These valuations have contributions that vary across horizons. We propose decompositions when the nature of this uncertainty is broadly conceived. By drawing on insights from decision theory, stochastic impulse response theory, and the pricing of uncertain cash flows, we provide novel characterizations. We use these methods to illustrate when and why uncertainty leads to more proactive policy approaches to climate change.

*This paper is an outgrowth of a previously circulated document entitled "How Should Climate Change Uncertainty Impact Social Valuation and Policy?". The authors thank Fernando Alvarez, Pengyu Chen, Adlai Fisher, Peter Hansen, Joanna Harris, Chun Hei Hung, Cosmin Ilut, Hagen Kim, Aleksei Oskolkov, Stavros Panageas, Diana Petrova, Eric Renault, Takis Souganidis, Grace Tsiang, and Judy Yue for helpful suggestions and Bin Cheng for exceptional research assistance. In addition, participants at the 2023 SITE Conference on Climate Finance, Innovation, and Challenges for Policy, the 2024 NBER Spring Asset Pricing Meeting, the 2024 Texas A&M Young Scholar Finance Consortium, and the 2024 SFS Cavalcade Annual Meeting provided valuable feedback. This research was supported in part by the University of Chicago Griffin Economics Incubator.

**University of Wisconsin and University of Missouri, Columbia
‡University of Chicago
*Arizona State University
‡‡Argonne National Laboratory

1 Introduction

Uncertainty, as it impacts prudent policy-making, often operates through multiple channels. We take climate change as our featured example. In our example economy we focus on four such channels:

i) *carbon-climate dynamics*: mapping from carbon emissions into temperature changes;

ii) *economic damage functions*: reductions in output because of changes in atmospheric temperature;

iii) *technological innovation*: future abatement cost reductions for CO_2-based energy through investment in research and development (R&D);

iv) *investment productivity*: exogenous shifts in the capital evolution that have persistent consequences.

The first three channels are explicitly linked to climate change and contribute to our analysis in specific ways. We include the fourth channel to provide a benchmark for comparison. By design, it captures the familiar "long-run risk" contributions to the macroeconomy in the absence of climate change. See, for example, Bansal and Yaron (2004) and the subsequent literature.

The design of prudent policies that limit climate change requires that we confront multiple aspects of uncertainty, some of which are difficult to gauge with full confidence. As Rising et al. (2022) have recently argued,

> The economic consequences of many of the complex risks associated with climate change cannot, however, currently be quantified. ... these unquantified, poorly understood and often deeply uncertain risks can and should be included in economic evaluations and decision-making processes.

While we do not take up the full challenge posed by uncertainties featured by Rising et al., we propose and implement methods for assessing the impact of uncertainty when the nature of this uncertainty is broadly conceived. These methods give one formal way to incorporate "deep uncertainty" into policy analyses. While our methods are more generally applicable, we apply them to an example economy with a climate change externality.

Although motivated in part by insights from the long-run risk literature, our contribution differs in two important ways. First, we explore the impact of the specific channels of uncertainty mentioned previously within an otherwise relatively simple production-based model. Second, we study valuation from a social perspective rather than a market perspective. These two perspectives differ because of production externalities induced by climate change. We adopt the social vantage point because climate change induced by human activity is at the forefront of many policy discussions. This social perspective provides a valuable benchmark for effectiveness of *ad hoc* policies implemented in market settings, including ones that currently exist and others that are proposed and viewed as politically feasible. While our application is to the design of robustly optimal policies, the uncertainty decompositions we propose and implement are more generally applicable. There is scope for such policies to be socially productive because of the failure of the "invisible hand," since market solutions do not account for the climate change externality.

We propose and implement methods for uncertainty decompositions when the nature of the uncertainty is broadly conceived. We push beyond the usual risk-based analyses by taking this broad approach to uncertainty, consistent with perspectives from multiple fields, including decision and control theory. These literatures formalize sagacious responses to alternative types of uncertainty, including *risk* within a model (unknown outcomes with known probabilities), *ambiguity* across models (unknown priors weighting alternative models or parameter configurations), and potential *model misspecification* (unknown flaws of fully specified probability models). The last of these three constructs gives a way to formulate concepts such as "deep uncertainty," or "radical uncertainty," that are present in policy discussions.

Prudent decision making is often linked to social valuations of endogenous state variables, including temperature and the stock of knowledge associated with targeted research and development (R&D). The resulting social valuations of endogenous state variables have contributions that are horizon-dependent as in the valuation of uncertain cash flow in equity pricing. We rely on decision theory formulations to explore the relative importance of alternative channels by which uncertainty impacts policy challenges. We extend tools from stochastic impulse response theory and from the pricing of uncertain cash flows to provide novel characterizations of the contributions to social valuations and their horizon-dependence.

Using our fictitious social planner setting, we provide a novel decomposition to assess which uncertainty components are most consequential for policy related to climate change. We solve alternative decision problems with different configurations of uncertainty, each featuring a specific source of the uncertainty. By varying the hypothetical exposure to the uncertainty, we show which of the four sources of uncertainty has the biggest impact on the prudent decisions of the planner. This decomposition has broader applicability to the investigation of uncertainty implications for prudent policy-making.

We also borrow and extend insights from asset pricing theory to study three assets: (i) capital used in producing aggregate output, (ii) the magnitude of global warming, which we measure using the temperature anomaly, and (iii) the knowledge capital from research and development targeted at developing new green technologies. We think of each of these as assets characterized by their implied intertemporal social cash flows. The asset price representations we use here depends on a "tilted probability" distribution that reflects aversion to model ambiguity or model misspecification. While much is made of measurements of the so-called social cost of carbon (SCC), quantifying the social value of R&D directed at the discovery of new and economically viable green technologies has received considerably less attention.[1]

Given our interest in social valuation, we show how to represent the marginal values of the endogenous states in terms of stochastic impulse responses to marginal changes in initial states that have uncertain consequences over alternative horizons and a social payoff at each horizon. Importantly, the social payoff includes a direct marginal utility contribution and marginal contributions to prospects of potentially big changes in either damages induced by more extreme values of climate change or in the technology opportunities for addressing climate change, both of which are depicted as Poisson events in our example economy.

We apply these methods to study the uncertain transition to a carbon-neutral economy. Our perspective on uncertainty is much broader than what is typical in economic analyses, but salient for problems like climate change. In addition to the familiar choice of capital investment, our planner has two other important decisions to make each period, how much carbon to emit and how much to invest in R&D. While both investment options have

[1]But even the social cost of global warming, a central input into the SCC, is altered by our inclusion of R&D investment in the toolkit of the social planner, modifying some of previous analyses in a substantive way.

uncertain outcomes, their social payoff implications are notably different. Specifically, the stochastic evolution of the stock of knowledge has an uncertain payoff horizon for the social payoff realized by removing the need for dirty energy in production of output. As is familiar from economic models of climate change, carbon emissions are both the flow outcome of an energy input into production, and a durable adverse contributor to future climate change. Through the first-order conditions, robustly optimal decisions depend on the social valuation of the corresponding assets. The Poisson components to our analysis provide a way for us to explore a trade-off between acting now or waiting for future uncertainty to be resolved in the future.

Analysis of our stylized model shows that technological innovation is the dominant uncertainty channel. For a prudent planning problem in our stylized environment, the socially and robustly efficient policy includes both immediate reductions in carbon emissions and a substantial investment in research and development (R&D). The planner reduces carbon emissions in the short run to limit damages and to allow for more time for R&D investments to be successful. Since uncertainty concerns highlight the technology innovation channel, we find that R&D investment is much more sensitive to uncertainty aversion than emissions reduction. Over what we suggest is an interesting range of uncertainty concerns, investment in R&D becomes all the more enhanced. To understand this result, we use an application of our novel asset pricing tools for social valuation to represent the social benefit of R&D as the expected discounted value of social payoffs using stochastic discount responses and a probability measure adjusted for concerns about model misspecification. This allows us to explain why, for this example economy, the fictitious social planner wants to be more proactive in the presence of more uncertainty about the time horizon over which the technology will become a successful replacement for fossil fuels.

1.1 Related literature

Several papers engage in uncertainty quantification by imitating approaches taken in the scientific literature. As a result, these assessments are done from the perspective of a planner who may unjustifiably ignore the uncertainty. This is in contrast to an external analyst who acknowledges this uncertainty and explores its ramifications. An important component of our analysis is to bring at least some of the uncertainty inside the decision problem of the

planner.

Some papers proceed by embracing a narrowly defined construct of risk (unknown outcomes with known probabilities) targeting the quantification of the social cost of carbon. See for instance, Cai et al. (2017), Bansal et al. (2019), and Hambel et al. (2021). While we embrace a more encompassing notion of uncertainty, some of our analysis could be reinterpreted from a pure risk perspective. For reasons that we will explain, we prefer the broader uncertainty vantage point. Kelly and Kolstad (1999) explore an explicit Bayesian learning approach in their stylized study of climate change uncertainty. While they show that endogenous learning evolves very slowly, they do not explore a policy maker with robust preferences over model misspecification and its impact. Weitzman (2009) uses a subjective expected utility approach to the study of damage uncertainty, also abstracting from robust preferences over model misspecification.

Broader notions of uncertainty have been considered in some of the prior climate-economics literature, including Hennlock (2009), Li et al. (2016), Lemoine and Traeger (2016), Barnett, Brock and Hansen (2020), Rudik (2020), Berger and Marinacci (2020), Barnett, Brock and Hansen (2022), and Barnett (2023). In contrast to this paper, the prior literature incorporating uncertainty concerns did not explore simultaneously the four channels of uncertainty that we do here, nor did it use asset pricing theory to provide revealing decomposition of the implied social valuations.[2] Moreover, we use an asset pricing perspective, extended to include broad uncertainty adjustments, to characterize the implied shadow asset values that support the prudent choices of the planner. Notably, the inclusion of R&D investment in the planner's policy choice set gives rise to some salient modifications of the uncertainty contribution to the social price of global warming as compared with previous analyses.

Previous work has explored the impact of technological innovation on economic and financial valuations, such as Bloom and Van Reenen (2002) and Kogan et al. (2017, 2020). Implications connected to climate change have been explored by Acemoglu et al. (2016) and Jaakkola and van der Ploeg (2019), among others. Our work, however, initiates the assessment of model uncertainty for the robustly optimal social investment in R&D.

A prominent strand of related literature has also examined investment under uncertainty,

[2]Barnett et al. (2020) also explored some standard asset pricing implications for a decentralization that supports a robustly optimal policy. But this prior analysis did not entertain an R&D investment choice nor did it develop the uncertainty decompositions that we describe here.

including Lucas Jr and Prescott (1971), Abel (1983), Dixit and Pindyck (1994), with recent contributions by Bloom et al. (2007), Novy-Marx (2007), and Bolton et al. (2019). The type of uncertainty considered in these settings is what we classify as risk, rather than concerns about potential misspecification as in our setting. Nevertheless, we find this earlier research on investment under uncertainty as a useful motivation for our construction of a benchmark model specification to which we include climate change considerations.[3]

1.2 Organization

The remainder of the paper proceeds as follows. Section 2 outlines the dynamic decision theory toolkit used for our uncertainty analysis and describes how this modifies the recursive optimization problem for our social planner. In Section 3 we construct asset pricing representations for the social valuations via marginal stochastic impulse responses as a function of the payoff horizon and marginal payoffs at each horizon. We show how to extend these representations to accommodate robustness to potential model misspecification and to include Poisson jumps with endogenous intensities. Since there are multiple components to the marginal payoffs, the asset pricing representations open the door to revealing decompositions coming from each of the components.

Sections 4 details the climate-economic modeling framework. Specifically, Section 4.1 describes the underlying economic production opportunities, abstracting from climate change; Section 4.2 presents the model of climate dynamics; Section 4.3 shows how these opportunities are reduced by global warming. Section 5 gives the intertemporal preferences of the hypothetical social planner. We construct the composite state vector in Section 6, show how the first-order conditions for maximization are related to value function derivatives, and describe how we compute the post-jump continuation value functions. We present quantitative results from an example economy in Section 7. Section 8 uses the asset pricing representation for the social value of the R&D knowledge capital to quantify the competing forces that contribute to the proactive R&D investment in the presence of enhanced concerns about uncertainty. Section 9 provides a sensitivity analysis for the planner preferences by considering changes in the subjective rate of discount and in the intertemporal elasticity of

[3]To allow for this modeling richness, we start with a very simple investment specification with adjustment costs.

substitution. Section 10 summarizes our conclusions and briefly comments on the value of new R&D investment.

2 Confronting uncertainty

We now analyze the contributions to the planner's Hamilton–Jacobi–Bellman (HJB) equation that emerge because of aversion to model misspecification. We pose our hypothetical social planner's decision problem in a continuous-time environment. The uncertainty adjustments for model misspecification concerns lead us to replace a recursive maximization problem with a two-player formulation where one player maximizes social well-being and the other adversarial player looks for baseline model or prior misspecifications with the most adverse consequences by solving a minimization problem. The uncertainty aversion of the social planner is reflected in penalties that limit the adversarial choice. In effect, this becomes a two-player zero sum game posed in continuous time with modifications to the HJB equations necessary to accommodate the uncertainty concerns. The analysis in this section focuses on the minimizing player and the implications for terms that enter the HJB equation involving the evolution of the value function. We temporarily omit the other terms, remembering that these are also important for deriving the maximizing control law.

To confront potential model misspecification, we follow Anderson et al. (2003) by entertaining misspecification linked both to the Brownian contribution and to the jump contribution. We use a well-studied construct called relative entropy or Kullback–Leibler divergence scaled by a penalty parameter to quantify misspecification. This divergence is measured as a non-negative expected log-likelihood ratio that we use to restrain the search over potential model discrepancies in the uncertainty analysis.

2.1 Brownian motion misspecification

Under a baseline probability specification, $W \stackrel{\text{def}}{=} \{W_t : t \geqslant 0\}$ is a multivariate standard Brownian motion, and $\mathfrak{F} \stackrel{\text{def}}{=} \{\mathfrak{F}_t : t \geqslant 0\}$ is the corresponding information filtration with $\mathfrak{F}_t$ generated information that is realized between dates zero and t. This information includes the Brownian increments that have been realized up to date t. Initially, we let $\mathfrak{F}$ be the Brownian filtration, but we subsequently will augment this filtration to include realizations

of jumps that will influence technology and damages induced by climate change.

As is familiar from derivative claims pricing, positive martingales with expectations equal to one parameterize changes in probability measures. From Girsanov theory, such martingales can be characterized by their implied drift distortions. In particular, under the martingale change in the probability measure, process $W \stackrel{\text{def}}{=} \{W_t : t \geqslant 0\}$ instead has a drift $H \stackrel{\text{def}}{=} \{H_t : t \geqslant 0\}$.

Suppose that the state vector process X has a local mean increment $\mu(X_t, A_t)dt$ and stochastic increment $\sigma(X_t, A_t)dW_t$, where A_t is a decision or action taken at time t. Throughout the essay we let lower-case variables capture potential realizations of random vectors. The realizations of the state vector, X_t, reside in a state space $\mathcal{X}$. For a value function, V, the drift or local mean of $V(X)$ is given by[4]

$$\frac{\partial V}{\partial x'}(X_t)\mu(X_t, A_t) + \frac{1}{2}\text{trace}\left[\sigma(X_t, A_t)'\frac{\partial^2 V}{\partial x \partial x'}(X_t)\sigma(X_t, A_t)\right]. \tag{1}$$

In this equation, we omit time dependence and think of V as the value function for an infinite horizon discounted problem. Formula (1) captures the time increment to risk confronted by the decision-maker.

The decision-maker entertains possible misspecification uncertainty by replacing formula (1) with the solution to

Problem 2.1.

$$\min_h \frac{\partial V}{\partial x'}(x)\left[\mu(x, a) + \sigma(x, a)h\right] + \frac{1}{2}\text{trace}\left[\sigma(x, a)'\frac{\partial^2 V}{\partial x \partial x'}(x)\sigma(x, a)\right] + \frac{\xi}{2}h'h$$

for a penalty parameter ξ.

The minimization captures a form of uncertainty aversion, analogous to risk aversion, since the minimizing objective will be less than or equal to (1). The penalty parameter ξ restrains the concern for robustness to model misspecification. The quadratic penalty in h is a local measure of "relative entropy" or Kulback–Leibler divergence.[5] A limiting choice of $\xi \approx \infty$ implies a minimizing choice of $h = 0$ with an implied contribution given by (1). Since the

[4]We use the notation $\frac{\partial V}{\partial x}(x)$ to denote a column vector of derivatives with respect to the column vector x and $\frac{\partial V}{\partial x'}(x)$ to be the corresponding row vectors of derivatives with respect to the row vector x'.

[5]For instance, see Anderson et al. (2003) for an elaboration.

minimization problem is quadratic in h, the minimizer is

$$h^* = -\frac{1}{\xi}\sigma(x,a)'\frac{\partial V}{\partial x}(x) \tag{2}$$

with a minimized objective:

$$\frac{\partial V}{\partial x'}(x)\mu(x,a) + \frac{1}{2}\text{trace}\left[\sigma(x,a)'\frac{\partial^2 V}{\partial x \partial x'}(x)\sigma(x,a)\right] - \frac{1}{2\xi}\frac{\partial V}{\partial x'}(x)\sigma(x,a)\sigma(x,a)'\frac{\partial V}{\partial x}(x).$$

Notice that the minimizing drift, h^*, is potentially state dependent. When σ depends on the action a, the drift of interest for valuation and interpretation depends on the maximizing action a expressed as a function of the state. The drift vector, h^*, has a relatively larger contribution when the value function is more adversely exposed to the Brownian increments. The parameter ξ governs the magnitude of the distortions. A smaller value of ξ results in drift adjustments with a larger magnitude.[6]

Remark 2.2. *As Anderson et al. (2003) emphasize, the negative implied drift distortions from a planner's problem are also the local shadow prices for concerns about misspecification. While they featured the case in which these shadow prices are also pertinent for competitive financial markets, the same insight carries over to social valuation in the presence of externalities that induce a wedge between market prices and social counterparts.*

2.2 Jump misspecification

Jump components play prominently in our uncertainty analysis. This is due to the inclusion of model ingredients that capture uncertainty tipping points that reveal magnitude and timing of damages to economic opportunities induced by climate change, as well as uncertainty in the arrival of a new, economically viable, green technology. The jumps depend on endogenously determined intensities that govern the probabilities of the jump realizations. Our specification of these intensities induces a corresponding endogeneity in the information structure.

We suppose there is a discrete set of jump states $\ell = 1, 2, ..., L$. Let $\mathcal{J}^\ell$ denote a state-dependent intensity for jump of type ℓ. Recall that the jump intensity, $\mathcal{J}^\ell$, implies an

[6]While this looks obvious from formula (2), it is a bit more subtle because the value function implicitly depends on ξ.

approximate jump probability, $\epsilon\mathcal{J}^\ell$, over a small time increment, ϵ. Following a jump of type ℓ, the value function jumps to V^ℓ. The jump process contributes the following term to the HJB equaiton for $V(X)$:

$$\sum_{\ell=1}^{L} \mathcal{J}^\ell(x)\left[V^\ell(x) - V(x)\right], \tag{3}$$

capturing the jump risk contribution to the decision problem.

To capture potential misspecification, we introduce a non-negative functions g^ℓ where the altered jump distribution has intensity $\mathcal{J}^\ell(x)g^\ell(x)$. To restrain the exploration of potential misspecification, we introduce a convex cost:

$$\xi \sum_{\ell=1}^{L} \mathcal{J}^\ell(x)\left[1 - g^\ell(x) + g^\ell(x)\log g^\ell(x)\right].$$

The term multiplying ξ is a local (in time) measure of relative entropy or Kullback–Leibler divergence applicable to jump processes.[7] To confront misspecification, we solve

Problem 2.3.

$$\begin{aligned}\min_{g^\ell \geqslant 0} \quad & \sum_{\ell=1}^{L} \mathcal{J}^\ell(x)g^\ell(x)\left[V^\ell(x) - V(x)\right] \\ & + \xi \sum_{\ell=1}^{L} \mathcal{J}^\ell(x)\left[1 - g^\ell(x) + g^\ell(x)\log g^\ell(x)\right].\end{aligned}$$

Minimization problem 2.3 has a quasi-analytical solution:

$$g^{\ell *}(x) = \exp\left(-\frac{1}{\xi}\left[V^\ell(x) - V(x)\right]\right), \tag{4}$$

with a minimized objective:

$$\xi \sum_{\ell}^{L} \mathcal{J}^\ell(x)\left[1 - \exp\left(-\frac{1}{\xi}\left[V^\ell(x) - V(x)\right]\right)\right], \tag{5}$$

which we use in place of (3). Notice from (4), that the distorted intensity is diminished when

[7] See, for instance, Anderson et al. (2003).

the jump in the continuation value function is larger, and conversely when the jump in the continuation value is smaller.

Remark 2.4. *In our example economy, we compute V^ℓ's by solving value functions conditioned on a damage jump ($\ell = 1, 2, ..., L-1$) or a technology jump ($\ell = L$) using the same baseline intensities for the remaining jump possibilities.*

Remark 2.5. *While we focus on misspecification aversion, as Hansen and Miao (2018) show, a mathematically similar but conceptually distinct adjustment can be made to accommodate ambiguity over the subjective weighting of alternative models.*

3 Asset pricing applied to social valuation

We construct a revealing asset pricing representation of marginal valuation captured by the derivative of a continuation value function with respect to an endogenous state variable. The derivatives play a central role in the first-order conditions for the robustly optimal controls. They also provide information in the analysis of the local policy responses emanating from a potentially sub-optimal allocation. This latter perspective is often embraced in public finance and underlies many, but not all, measurements of the social cost of carbon featured in climate change analyses. In our application, these marginal valuations can be interpreted as a social cost of climate change or a social return to research and development.

A central ingredient in our representations are marginal stochastic impulse responses. Our stochastic models are nonlinear which renders the commonly-used impulse response methods inapplicable. For linear stochastic models, global responses are scaled versions of marginal responses. In our nonlinear stochastic environments, we use marginal responses. We feature marginal valuation responses to alternative changes in endogenous state variables. As we will see, our representations open the door to value decompositions that help us to explore and interpret our findings.

We produce calculations that include two features that are important for our analysis. First, as in the previous section, we allow for forms of uncertainty aversion that extend beyond standard risk aversion characterizations. This broader perspective will be captured as an uncertainty-adjusted probability measure along the lines of Barnett et al. (2020). Second, we allow for stochastic terminal contributions that can depend on endogenous state

variables. These terminal conditions are reflected in changes in continuation values induced by Poisson events or jumps. The continuation values in our application are computed as described in Remark 2.4. In summary, our "asset pricing representation" has the following components:

i) a vector of stochastic impulse responses that inform us how a marginal change in an initial state variable influences an entire vector of future state variables over alternative horizons;

ii) a vector of potential marginal payoffs in future time periods specified as functions of future state variables.

Contribution i) introduces a form of stochastic discounting into our analysis. Contribution ii) gives a vector of marginal payoffs depicted as cash flows. These include direct marginal utility contributions and contributions that come from the Poisson events that might be realized at any point in time. In what follows, we provide formal constructions of each of these contributions. Moreover, they lead us to provide horizon characterizations of the magnitudes of the alternative contributions similar to standard impulse response applications. The horizon characterizations are similar to cash flow asset pricing decompositions used in the study of equity market pricing.

3.1 Pre-jump stochastic dynamics

As a part of a more general derivation, we begin with state dynamics modeled as a Markov diffusion:

$$dX_t = \mu(X_t)dt + \sigma(X_t)dW_t$$

These dynamics could be the outcome of an optimization problem or they could be perhaps the socially inefficient outcome of a market equilibrium. Consider the evaluation of discounted utility where the instantaneous contribution is $U(x)$, where x is the realization

of a state vector X_t. The function V is known to satisfy a Feynman-Kac (FK) equation:

$$\begin{aligned} 0 &= \delta U(x) - \delta V(x) + \mu(x) \cdot \frac{\partial V}{\partial x}(x) + \frac{1}{2}\text{trace}\left[\sigma(x)' \frac{\partial^2 V}{\partial x \partial x'}(x)\sigma(x)\right] \\ &\quad + \sum_{\ell=1}^{L} \mathcal{J}^{\ell}(x)\left[V^{\ell}(x) - V(x)\right] \end{aligned} \tag{6}$$

for a given collection of "terminal" value functions, V^{ℓ} for $\ell = 1, 2, ..., L$. These are post jump value functions that are computed in advance of solving for V. Then V satisfies the forward-looking equation:

$$V(X_0) = \mathbb{E}\left[\int_0^{\infty} Dis_t \left[U(X_t) + \sum_{\ell=1}^{L} \mathcal{J}^{\ell}(x) V^{\ell}(x)\right] \mid X_0\right] \tag{7}$$

where Dis contributes a state-dependent discount rate:

$$Dis_t \stackrel{\text{def}}{=} \exp\left(-\int_0^t \left[\delta + \sum_{\ell=1}^{L} \mathcal{J}^{\ell}(X_u)\right] du\right), \tag{8}$$

The process Dis includes both an adjustment for the probability that a jump has not occurred given by:

$$\exp\left(-\int_0^t \left[\sum_{\ell=1}^{L} \mathcal{J}^{\ell}(X_u)\right] du\right)$$

along with the usual exponential contribution $\exp(-\delta t)$. The flow term being discounted in formula (7) include both a direct utility contribution and a continuation-value contribution should a jump take place.

We want to represent:

$$V_{x_i}(x) \stackrel{\text{def}}{=} \frac{\partial V}{\partial x_i}(x)$$

as an expected discounted value of a marginal impulse responses of future X_t to a marginal change of the i^{th} coordinate of x.

3.2 Variational process

As in Borovička et al. (2014) we construct marginal impulse response functions using what are called variational processes. Following Fournie et al. (1999), we form the first variational process, M, that gives the marginal impact on future X of a marginal change in one of the initial states. Thus this process has the same dimension as the number of components of X. By initializing the process at one of the alternative coordinate vectors we determine the initial state of interest.[8]

The drift for the i^{th} component of M is given by

$$m' \frac{\partial \mu_i}{\partial x}(x)$$

and the coefficient on the Brownian increment is given by

$$m' \frac{\partial \sigma_i}{\partial x}(x)$$

for m a hypothetical realization of M_t and x a hypothetical realization of X_t where $'$ denotes vector or matrix transposition. The implied evolution of the process M^i is given by

$$dM_t^i = (M_t)' \frac{\partial \mu_i}{\partial x}(X_t)dt + (M_t)' \frac{\partial \sigma_i}{\partial x}(X_t)dW_t.$$

The drift for the composite process (X, M) is given by:

$$\hat{\mu}(x, m) \stackrel{\text{def}}{=} \begin{bmatrix} \mu(x) \\ m' \frac{\partial \mu_1}{\partial x}(x) \\ ... \\ m' \frac{\partial \mu_n}{\partial x}(x) \end{bmatrix}, \tag{9}$$

[8]Our initial condition for M_0 differs from Fournie et al. (1999) in a superficial way. They treat M as a matrix with an identity as the initialization. In this way they consider all of the states of interest simultaneously. We take M to be a vector and characterize the marginal initial responses one at a time by letting the initial condition be any one of the coordinate vectors.

and the composite matrix coefficient on dW_t is given by

$$\hat{\sigma}(x,m) \stackrel{\text{def}}{=} \begin{bmatrix} \sigma(x) \\ m' \frac{\partial \sigma_1}{\partial x}(x) \\ \cdots \\ m' \frac{\partial \sigma_n}{\partial x}(x) \end{bmatrix}. \tag{10}$$

With these constructions, we now write the composite dynamics as:

$$\begin{bmatrix} dX_t \\ dM_t \end{bmatrix} = \hat{\mu}(X_t, M_t)dt + \hat{\sigma}(X_t, M_t)dW_t.$$

By initializing M_0 at a coordinate vector in $\mathbb{R}^n$ with a one in position i, we obtain the vector M_t of stochastic responses to a marginal change in the i^{th} component of the state vector X_0. In our application, we simulate the M process using these stochastic dynamics.

3.3 Marginal valuation

By differentiating the Feynman-Kac equation (6) with respect to each coordinate, we obtain a vector of equations, one for each state variable. We then form the dot product of this vector system with respect to m to obtain a scalar equation system that is of particular interest. The resulting equation turns out to also be a FK equation for the function:

$$m \cdot \frac{\partial V}{\partial x}(x)$$

as established in the Appendix B. Given that the equation to be solved involves both m and x, this equation uses the diffusion dynamics for the joint process (X, M).

The solution to this derived Feynman-Kac equation is of the form of a discounted expected value:

$$\frac{\partial V}{\partial x}(X_0) \cdot M_0 = \mathbb{E}\left[\int_0^\infty Dis_t\left(M_t \cdot Scf_t\right) \mid X_0, M_0\right] \tag{11}$$

where Dis is given by (8), and Scf is a social cash flow vector given as:

$$Scf_t \stackrel{\text{def}}{=} \delta U_x(X_t) + \sum_{\ell=1}^{L} \mathcal{J}_x^\ell(X_t)\left[V^\ell(X_t) - V(X_t)\right] + \sum_{\ell=1}^{L} \mathcal{J}^\ell(X_t) V_x^\ell(X_t).$$

where U_x and $\mathcal{J}_x^\ell$ for $\ell = 1, .., L$ are vectors of partial derivatives with respect the state vector x. By initializing the state vector M_0 to be a coordinate vector of zeros in all entries but entry i we obtain the formula of interest.

The social cash flow process, Scf has three terms to be discounted, two of which come from the possibilities of jumps to new continuation values. The marginal response process, M, acts as an additional stochastic adjustment to valuation. In effect, there is a composite stochastic discount vector process $DisM$ applied component-by-component to the state vector. Notice that the cash-flow process can be decomposed additively into a direct utility contribution and contribution for each of the potential jumps.

In our application, we report contributions for each time horizon and for each jump component along with the direct utility contribution:

$$\begin{aligned}
&\delta\mathbb{E}\left[Dist_t M_t \cdot U_x(X_t) \mid X_0, M_0\right] \\
&\mathbb{E}\left[Dist_t M_t \cdot \mathcal{J}_x^\ell(X_t)\left[V^\ell(X_t) - V(X_t)\right] \mid X_0, M_0\right] \\
&\mathbb{E}\left[Dist_t M_t \cdot V_x^\ell(X_t)\mathcal{J}^\ell(X_t) \mid X_0, M_0\right]
\end{aligned}$$

for $t \geqslant 0$ and $\ell = 1, ..., L$. These provide valuation counterparts to impulse responses commonly reported in economic dynamics. The initialization of M_0 dictates the marginal change under consideration.

Remark 3.1. *Notice that the components of Scf_t given by:*

$$\delta U_x(X_t) + \sum_{\ell=1}^{L} \mathcal{J}_x^\ell(X_t)V^\ell(X_t) + \sum_{\ell=1}^{L} \mathcal{J}^\ell(X_t)V_x^\ell(X_t)$$

come from differentiating the stochastic flow contribution of (7) *with respect to the state vector. The additional component:*

$$-\sum_{\ell=1}^{L} \mathcal{J}_x^\ell(X_t)V(X_t)$$

is present because altering the state at date t changes the jump probabilities and hence the discouting. The value function V emerges as a convenient way to capture this forward looking-impact. Note that $V(X_t)$ can be expressed using formula (7) *shifted forward to date t. Anal-*

ogous forward-looking formulas apply to post-jump continuation values, V^ℓ, although these are computed in advance and are based on different jump possibilities.

Remark 3.2. *Fournie et al. (1999) use these types of methods to produce measurement of the sensitivity of derivative claims prices to inputs. But we have not seen these techniques developed and applied in the setting of stochastic optimal control. Moreover, we extend these methods to allow for uncertainties, broadly conceived, along with revealing decompositions.*

3.4 Incorporating robustness

To incorporate robustness, we use the expectation associated with the stochastic dynamics induced by the minimizing h and g^ℓ's. We let $g^{\ell *}$ denote the latter minimizer for $\ell = 1, 2, ...L$. We obtain a formula analogous to that of (11):

$$\frac{\partial V}{\partial x}(X_0) \cdot M_0 = \widetilde{\mathbb{E}}\left[\int_0^\infty Dis_t \left(M_t \cdot Scf_t\right) \mid X_0, M_0\right]$$

where the expectation $\widetilde{\mathbb{E}}$ uses the diffusion dynamics incorporating the minimizing drift distortions, h^* implied by robustness. In addition, we modify the discount factor term to be:

$$Dis_t \stackrel{\text{def}}{=} \exp\left(-\int_0^t \left[\delta + \sum_{\ell=1}^L \mathcal{J}^\ell(X_\tau) g^{\ell *}(X_\tau)\right] d\tau\right),$$

and the flow term:

$$\begin{aligned} Scf_t \stackrel{\text{def}}{=} \delta U_x(X_t) &+ \sum_{\ell=1}^L \mathcal{J}_x^\ell(X_t) g^{\ell *}(X_t) \left[V^\ell(X_t) - V(X_t)\right] \\ &+ \sum_{\ell=1}^L \mathcal{J}^\ell(X_t) g^{\ell *}(X_t) V_x^\ell(X_t) \\ &+ \xi \sum_{\ell=1}^L \mathcal{J}_x^\ell(X_t) \left[1 - g^{\ell *}(X_t) + g^{\ell *}(X_t) \log g^{\ell *}(X_t)\right]. \end{aligned} \tag{12}$$

Notice that we have scaled each intensity or its partial derivative by the corresponding $g^{\ell *}$ with the exception of the fourth contribution to the flow term. This fourth term is included because marginal changes in the state vector alter the exposure to uncertainty and thus im-

pacts valuation. While partial derivatives with respect to the intensities $\mathcal{J}^\ell$ contribute to the second term in Scf, there is no counterpart from the jump distortion, $g^{\ell *}$. We may treat this robust probability adjustment as exogenous to the decision maker and hence not impacted by endogenous state vector components. As is verified in the appendix, this treatment is a ramification of the minimization (via application of the Envelope Theorem).

As we have seen, an extra unit of each asset or state variable in a dynamical system sets off a marginal impulse response function from the initial shock date to the future. Applying a technical toolkit which includes Feynman-Kac equations and first variation processes, our valuation techniques enable us to derive the price of these marginal changes as the conditional expectation of the sum of appropriately discounted marginal responses of the asset under scrutiny set off by an incremental change in the initial state.

In the application that follows, our representations allow for an assessment of the various components of the social valuations of economic capital, R&D knowledge stock, and temperature state variables in such a coupled geophysical economic system. Our techniques provide valuations when allowing for uncertainty broadly conceived. In our setting, this includes concerns by the planner about misspecification of the diffusion and jump processes governing the endogenous evolution of the asset stocks in the model. As a result, our techniques provide valuation of each layer of uncertainty by decomposing the asset valuation contribution from each layer of uncertainty relative to when that layer is absent.

4 Example economy

We now consider a simple production-based model with an AK production technology subject to adjustment costs. By design, this formulation has close ties to much of the long-run risk literature with exogenously specified consumption endowments. Prior to introducing climate change, we include three modifications. First, we consider an adjustment cost version of an AK model. This allows us to consider a baseline environment with a conventional investment option. Second, we include an energy input in a way that is mathematically similar to what is used in "DICE" models as developed by Nordhaus (2017) and others. Our rationale for this specification is a bit different leading us to different parameter settings. Third, we allow for a second investment option, which is R&D that could eventually remove the need for energy input. With regard to the second modification, some suggest that an economically

viable version of nuclear fusion might achieve this aim.[9] In particular, our decision maker (social planner) has two investment opportunities given our two forms of capital: one is our broad-based notion of a aggregate capital stock, and the other is the stock of R&D devoted to the discovery of a new green technology. The costs of these investments by design will be the same, but the payoffs in production will be quite different.

4.1 Production and innovation

The economic component of our model has two endogenous state variables: the stock of productive capital, K_t, and the stock of R&D capital, R_t.

4.1.1 Output

Output is split between consumption and two different types of investment with distinct intertemporal contributions to production: a conventional capital investment, I_t^k, and an investment in R&D, I_t^r (the superscripts denote the investment type):

$$C_t + I_t^k + I_t^r = \alpha K_t \left(1 - \phi_0(Z_t) \left(A_t^b\right)^{\phi_1}\right) \tag{13}$$

for $\phi_1 \geqslant 2$ and $0 < \phi_0(Z_t) \leqslant 1$, where

$$A_t^b \stackrel{\text{def}}{=} \left(1 - \frac{\mathcal{E}_t}{\beta \alpha K_t}\right) \mathbf{1}_{\{\mathcal{E}_t < \beta \alpha K_t\}}, \tag{14}$$

and $\mathbf{1}$ is an indicator function that assigns one to the event in the $\{\cdot\}$ brackets. The jump process Z has an evolution which will be described subsequently.

Emissions $\mathcal{E}_t$ are a proxy for a "dirty" energy input into production.[10] When emissions fall short of the threshold $\beta \alpha K_t$, there is a corresponding convex adjustment in the output given by the right-hand side of (13). This technology is, by design, homogeneous of degree one. For a fixed K_t, the implied production function is flat when emissions exceed the threshold of $\beta \alpha K_t$ and has a zero left derivative at this point. The function equals $1 - \phi_0(Z_t)$ when

[9] See Chang (2022) and Stalard (2024) for a recent discussions of progress in the development of an economically viable nuclear fusion technology.

[10] While we could include A_t^b as an entry in the control vector, A_t, this is unnecessary because A_t^b is fully determined by emissions and capital.

$\mathcal{E}_t = 0$ and increases up the threshold as a concave function with curvature dictated by the parameter ϕ_1. We feature the case in which $\phi_1 = 3$.

Remark 4.1. *This type of mathematical formulation has showed up in many climate-economics papers since the work of Nordhaus. See, for instance, Nordhaus (2017). The term*

$$\phi_0(Z_t)\left(A_t^b\right)^{\phi_1}$$

is commonly referred to as an abatement cost, perhaps even a cost that is external to the firm. This, however, is only a "cost" in our specification relative to a technology that does not require emissions. The right-hand side of relation (13) *shows output increasing in $\mathcal{E}_t$ until it reaches a threshold $\beta\alpha K_t$, after which additional emissions are unnecessary as capital is the constraining factor. Embedding this $\mathcal{E}_t \geqslant \beta\alpha K_t$ implication in a fixed-proportion technology for emissions lower than $\beta\alpha K_t$, corresponds to setting $\phi_0(Z_t) = 1$ and $\phi_1 = 1$. By increasing ϕ_1 we increase the production possibilities, as does lowering $\phi_0(Z_t)$. In light of this, we view the right-hand side of* (13) *as a production relation without reference to an "abatement cost." This, of course, is a matter of interpretation, but it also impacts how we think of plausible calibrations of $\phi_o(Z_t)$.*[11] *We will have more to say about this subsequently.*

We suppose initially that $\phi_0(Z_t) > 0$ and that at some point in the future a fully green technology becomes economically viable, in which case $\phi_0(Z_t) = 0$ and dirty energy is no longer needed to produce output. For instance, think of a substantial advance such as nuclear fusion.[12] Investment in R&D makes this discovery more likely. Specifically, the jump to the clean technology is governed by a Poisson intensity $\mathcal{J}^L(R_t) = R_t$.

4.1.2 Productive capital evolution

The stock of productive capital, K_t, evolves as

$$dK_t = K_t\left(-\mu_k + \frac{I_t^k}{K_t} - \frac{\kappa}{2}\left(\frac{I_t^k}{K_t}\right)^2\right)dt + K_t\sigma_k dW_t,$$

[11] See Appendix A.3 for a further discussion based on computing first and second derivatives of a proposed production function.

[12] See Chang (2022) for a recent discussion of the state of this technology and its promise.

where σ_k is a row vector with the same dimension as the underlying Brownian motion. New investment, I_t^k, augments the capital stock, K_t, subject to an adjustment cost captured by the curvature parameter κ. Capital is broadly conceived to include human capital and intangible capital.

4.1.3 R&D capital evolution

A process R captures the stock of R&D-induced knowledge capital and evolves as

$$dR_t = -\zeta R_t dt + \psi_0 \left(I_t^r\right)^{\psi_1} \left(R_t\right)^{1-\psi_1} dt + R_t \sigma_r dW_t, \tag{15}$$

where $0 < \psi_1 < 1$ and I_t^r is an investment in research and development. While we will solve a social planner's problem, this evolution equation potentially includes an externality associated with R&D. For pedagogical simplicity, we consider the case of a single technology jump to a fully productive green technology. The parameter ζ captures potential depreciation in the stock of knowledge pertinent for future technological progress. The term $\sigma_r dW_t$ reflects an exogenous stochastic inflow of information about the future likelihood of a technological advance.[13]

4.2 Climate dynamics

Here we follow the simplified climate dynamics used in Brock and Xepapadeas (2017) and Barnett, Brock and Hansen (2022). Their approach is based on an approximation from the geoscience literature used to support model comparisons. Specifically, Matthews et al. (2009) and others have purposefully constructed an approximation for climate model output:

$$\text{temperature anomaly } (Y_t) \approx \text{ TCRE}(\theta) \times \text{ cumulative emissions },$$

where TCRE is an acronym for the **T**ransient **C**limate **R**esponse to cumulative **E**missions. This simplified formulation abstracts from transitory "weather" fluctuations in temperature. Instead, emissions today have a long-lasting impact on temperature in the future where TCRE is a measure of climate sensitivity.

[13]For a recent exploration of the policy implications of R&D for a green breakthrough technology, see Jaakkola and van der Ploeg (2019).

Our specific form is given by

$$dY_t = \mathcal{E}_t[\bar{\theta}dt + \varsigma dW_t]$$

where $\bar{\theta}$ is the equally weighted average of the $\theta(i)$'s where each $\theta(i)$ is a TCRE obtained from the set Θ of TCRE's implied by alternative climate models. The term ςdW_t captures short time scale fluctuations. Figure 1 gives a histogram of the θ's that we use in our computations, which are constructed using pulse experiments applied to models of carbon and climate dynamics from the climate science literature. Appendix A.1 describes how we constructed this histogram.[14] For baseline probabilities across the alternative climate models, we presume that each model has the same subjective probability We abstract from parameter learning since learning about such parameters has been slow.[15]

[14] As is well known from the climate science literature, the models actually imply an emissions response that builds from zero to a peak effect in about ten years followed by an approximate flattening at heterogeneous values. See Ricke and Caldeira (2014) for a discussion of these findings. Roughly speaking, the heterogeneous values at which the responses flatten out are equal to the model-specific TCRE's that we use. As we argue in Barnett et al. (2022), these transient dynamics have little impact on the model's implications for policy. Thus here we adopt this simpler specification to avoid having to include an additional state variable.

[15] One could imagine that in the future observations on more extreme temperatures could result in learning becoming more evident.

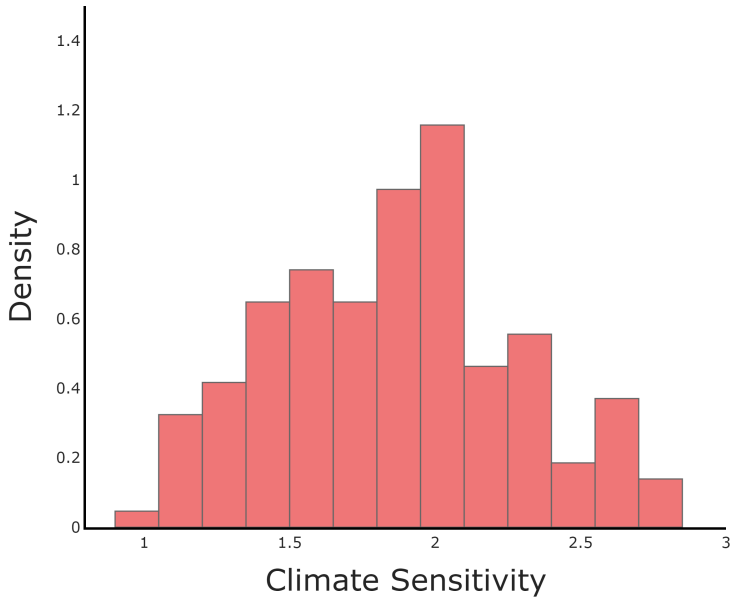

Figure 1: Histograms for the exponentially weighted average responses of temperature to an emissions pulse from 144 different models using a rate $\delta = .01$.

4.3 Damages to economic opportunities

We assume that capital, output, both investments, and consumption are all diminished proportionately by N_t. Our damage specification uses a piecewise log quadratic specification as a function of the temperature anomaly y. We suppose that the derivative of the logarithm of damages $\hat{n}$ with respect to the temperature anomaly is

$$\begin{aligned} \frac{d\hat{n}}{dy} &= \lambda_1 + \lambda_2 y & y \leqslant \tilde{y} \\ \frac{d\hat{n}}{dy} &= \lambda_1 + \lambda_2 \left(y - \tilde{y} + \bar{y}\right) + \lambda_3(\ell)(y - \tilde{y}) & y > \tilde{y} \end{aligned} \tag{16}$$

for $\ell = 1, ..., L-1$. This equation has an initial condition $\hat{n}(0) = 0$. In the stochastic version of what follows, $\tilde{y}$ will be triggered by a Poisson jump prior to a temperature threshold $\bar{y}$. We specify the intensity so that this jump takes place in the interval $[\underline{y}, \bar{y}]$. We shift the derivative of damages with respect to temperature to the right as captured by the change from $\lambda_2 y$ to $\lambda_2 \bar{y}$. We also increase the slope by including a term $\lambda_3(\ell)(y - \tilde{y})$, where the

coefficient $\lambda_3(\ell)$ is *ex ante* uncertain.

In Figure 2 we plot the implied damage functions for thresholds $\tilde{y} = 1.5$ and $\tilde{y} = 2$. These two thresholds are often referred to in discussions of the consequences of climate change. Each of the plots includes a range of $\lambda_3(\ell)$'s used in our quantitative policy assessment. The plotted solutions use the formula in Appendix A.2.[16]

As we mentioned previously, there has been considerable heterogeneity in the damage functions used in climate-economic models including a recognition that the curvature is best viewed as uncertain. One *ex ante* reasonable approach would be to activate learning over time about this curvature based on future information.[17] While conceptually appealing (and computationally challenging), we find this stylized approach well suited to capture a situation in which learning is slow now but could be much accelerated once damages become more severe. Since the jump intensity depends on the temperature anomaly, like learning, this dependence introduces a mechanism by which emissions impact information available to the decision maker. Importantly, this allows us to explore the trade-off between acting now versus waiting until more information is available.

[16]There are plots for a very similar differential specification in Barnett et al. (2022). Our interpretation of common equations differs, which changes the solutions being plotted. Their construction results in discontinuous damage functions and potential discrete jumps in the damages. Under our construction, the level of damages does not jump at the time of the Poisson event.

[17]Rudik (2020) has a comprehensive treatment of learning and robustness to misspecification within the context of damage function uncertainty. To make this tractable, the unknown damage parameters are learned from a regression of aggregate output growth, absent damages, onto temperature. This type of exercise may open the door to a more comprehensive treatment of learning and a more targeted robustness analysis expressed in terms of prior/posterior ambiguity. Rudik (2020) featured only one of the four uncertainty channels that we investigate in this paper.

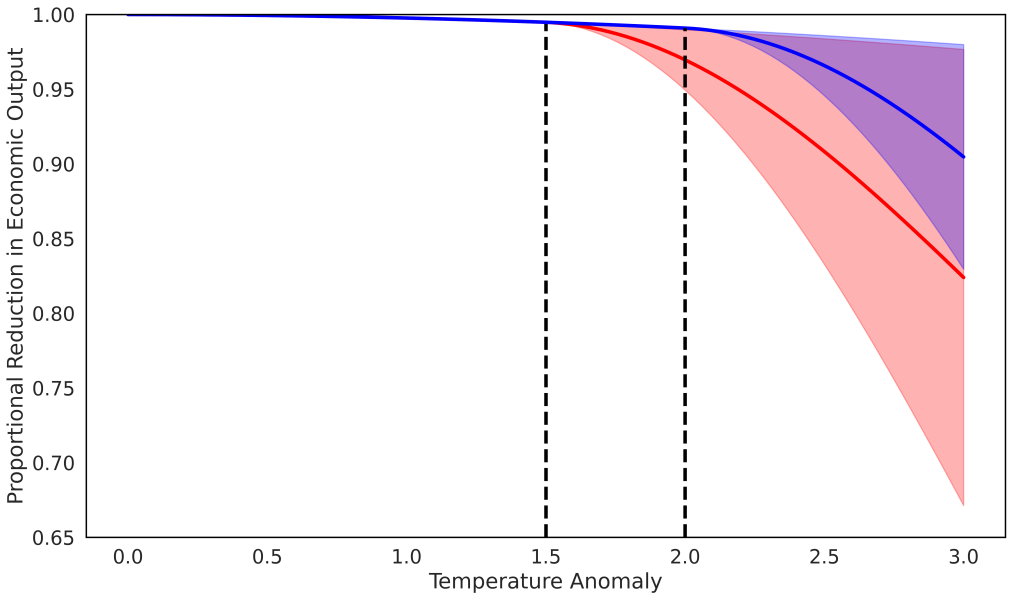

Figure 2: Range of possible damage functions for two cases with different jump thresholds. The solid lines show the average values, and the shaded regions give the range of possible values for $\exp(-n)$, which measures the proportional reduction of the productive capacity of the economy. The blue line and region show the damage function curvature when the jump occurs at $Y_t = \bar{y} = 2.0$. The red line and region show the damage function curvature when the jump occurs at $Y_t = \underline{y} = 1.5$. The black dashed lines indicate the values of Y_t for the upper and lower jump thresholds for the temperature anomalies.

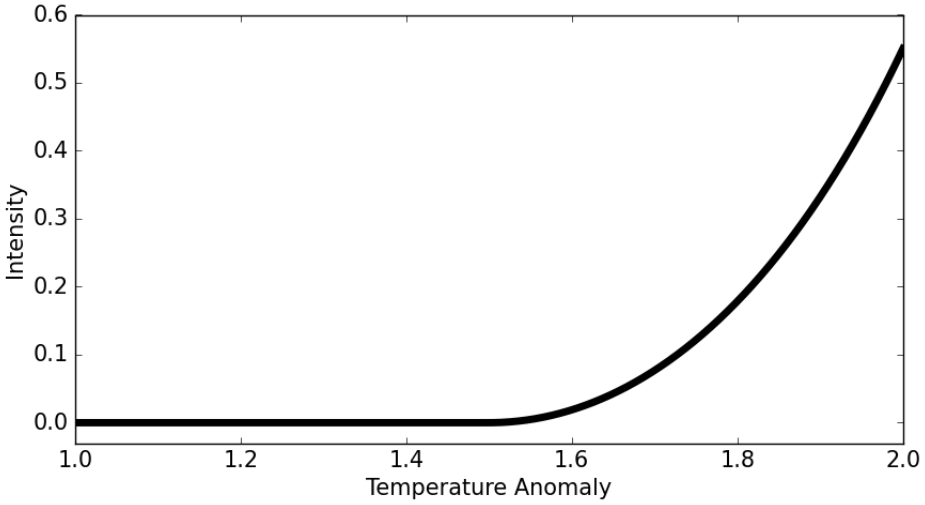

Figure 3: Plot of the intensity function given by $\mathcal{J}^n = r_1 \left(\exp\left(\frac{r_2}{2}(y-\underline{y})^2\right) - 1\right) \mathbf{1}_{\mathbf{y} \geqslant \underline{\mathbf{y}}}$ with $r_1 = 1.5$ and $r_2 = 2.5$. The implied probability of a jump at an anomaly of 1.6 is approximately .02 per annum, increasing to about .08 per annum at an anomaly of 1.7, increasing further to approximately .18 per annum at an anomaly of 1.8 and then to about one-third per annum when the anomaly is 1.9.

As a second source of uncertainty, the jump triggers a move to a possibly more concave region of the damage function rather than a simplistic tipping point with an instantaneous disaster. This incremental concavity is uncertain *ex ante* but known to the planner once the jump takes place. Prior to the jump, we represent each possible value $\lambda_3(\ell)$ for $\ell = 1, 2, ..., L-1$. with a baseline initial probability distribution π_ℓ. The jump-specific instensities are

$$\mathcal{J}^\ell(y) = \left(\frac{1}{L-1}\right) \mathcal{J}^n(y), \;\; \ell = 1, ..., L-1.$$

The implied damage evolution has two branches for the baseline stochastic evolution, one prior to a jump and another after the jump. Suppose the jump occurs at $t = \tau$ with realization ℓ. Then

$$d \log N_t = \begin{cases} \left(\lambda_1 + \lambda_2 Y_t\right) \mathcal{E}_t \left[\bar{\theta} dt + \varsigma dW_t\right] + \frac{\lambda_2 |\varsigma|^2 (\mathcal{E}_t)^2}{2} dt & t \leqslant \tau \\ \left[\lambda_1 + \lambda_2 \widehat{Y}_t + \lambda_3\left(\ell\right)\left(\widehat{Y}_t - \bar{y}\right)\right] \mathcal{E}_t \left[\bar{\theta} dt + \varsigma dW_t\right] & \\ \quad + \frac{[\lambda_2 + \lambda_3(\ell)] |\varsigma|^2 (\mathcal{E}_t)^2}{2} dt & t > \tau, \end{cases}$$

for $\widehat{Y}_\tau = \bar{y}$.

Remark 4.2. *As posed, our model is at the global scale. Note that our specification of a jump in damages induces a jump in the continuation values that we determine endogenously. This jump could be thought of as a "tipping point" in the continuation values that triggers a move to a more concave region of the damage function. Knowledge of this additional concavity is sufficient to induce a shift in the continuation value function. This curvature could be dictated by economic damages or by additional climate damages triggered by a temperature change.*

Existence of global scale tipping points is controversial within the climate literature. For example, see Brook et al. (2013) and Levitan (2013). We suspect that lower-order tipping points become a more salient concern for extended versions of the analysis with regional heterogeneity in the exposure to climate change. We intend our specification of damages only to be an initial platform for addressing the layers of important uncertainties in climate damages and prudent society responses. We find this to be more appealing than the so-called carbon-budgeting approach that imposes a Hotelling-type constraint on emissions to avoid crossing a temperature threshold.[18]

Remark 4.3. *The planner cares about the conditional mean of the $\theta(i)$'s, which we take to be $\bar{\theta}$ and explores the potential distortions of this mean. In what follows, we report the minimum relative entropy distortion of this by minimizing*

$$\sum_{i=1}^{I} \pi_i \left(\log \pi_i + \log I\right) \tag{17}$$

subject to a mean constraint and a constraint that the $\pi(i)$'s sum to unity.

As an alternative approach, we could adopt an ambiguity averse formulation with a distinct penalization obtained by adding a second penalty term that scale the relative entropy term in (17) *by a positive coefficient.*[19] *One advantage of the current approach is that there is a single penalty parameter we can compare more directly alternative channels of uncertainty.*

[18] Setting a carbon budget in terms of cumulative emissions typically abstracts from the inherent uncertainty in how emissions impact temperature. When it's taken to be a hard constraint, the implied damages when the constraint binds immediately become very substantial in contrast to damage function specifications like ours and others engaged in climate-economic research.

[19] See Appendix A.5 for an elaboration.

5 Social planner preferences

We adopt a recursive representation of preferences in continuous time for the planner. We start by forming the continuation value under risk for each calendar date, t as follows:

$$\begin{aligned} V_t &= \delta \int_0^\infty \mathbb{E}\left[\exp(-\delta\tau)\left(\log C_{t+u}\right) \mid \mathfrak{F}_0\right] du \\ &= \delta \int_0^\tau \mathbb{E}\left[\exp(-\delta u)\left(\log C_{t+u}\right) du \mid \mathfrak{F}_0\right] + \exp(-\delta\tau)\mathbb{E}\left(V_{t+\tau} \mid \mathfrak{F}_t\right). \end{aligned}$$

where $\mathfrak{F}_t$ reflects the date t information available to the planner. The second equality expresses a backward recursion linking future continuation values to the current one. The following differential equation gives the local representation:

$$0 = \delta\left(\log C_t - V_t\right) + \lim_{\epsilon \downarrow 0} \frac{1}{\tau}\left[\mathbb{E}\left(V_{t+\tau} - V_t \mid \mathfrak{F}_t\right)\right]. \tag{18}$$

This equation becomes a Hamilton-Jacobi-Bellman (HJB) equation once we substitute a candidate value function expressed as a function of the state vector. With a minor abuse of notation, $V_t = V(X_t)$.

5.1 Misspecification aversion

The HJB equations that interest us include maximization along with the aversion adjustments captured by minimization. Specifically, when solving our planner's robust decision problem, we embed subproblems 2.1 and 2.3 inside our HJB equations. Thus the robustness adjustments we derived in Section 2 replace the local mean of the continuation value implied by the candidate value function.

Remark 5.1. *Model misspecification aversion is mathematically equivalent to risk aversion in a recursive utility formulation obtained by setting the risk version parameter, γ, as*

$$\gamma = \frac{1+\xi}{\xi}$$

This insight holds for discrete-time specifications within the class studied by Kreps and Porteus (1978) and Epstein and Zin (1989). It also carries over to continuous-time recursive

utility as in Duffie and Epstein (1992), extended to include jump risk.[20] *This equivalence will not carry over for some of uncertainty decompositions that we explore and so will break down for many of our computations.*

The representation deduced in this section assumes a unitary elasticity of substitution which we feature in most of our computations, although we do explore sensitivity to this modeling choice. In Appendix A.4 we describe the extension allowing for other values of this substitution parameter. The change also has ramifications for the asset pricing formulas we deduced in Section 3.

Remark 5.2. *While we have denoted the continuation value dynamics presuming C is consumption, the actual consumption in our model is C/N since climate change induces proportional reduction in macroeconomic aggregates. We make this adjustment in what follows.*

5.2 A robustness decomposition

One focal point of our analysis will be the quantitative assessment of alternative channels of uncertainty. To do so, we start by computing solutions to two benchmark problems used as bases for comparison. One is a planner's problem that imposes what Cerreia-Vioglio et al. (2021) refer to as "misspecification neutrality." Formally this is achieved by imposing $\xi = \infty$. The second imposes a finite ξ entertaining misspecification of all four channels within our example economy:

i) *carbon-climate dynamics*: mapping from carbon emissions into temperature changes;

ii) *economic damage functions*: reductions in output because of changes in atmospheric temperature;

iii) *technological innovation*: future abatement cost reductions for CO_2-based energy through investment in research and development (R&D);

[20] This mathematical equivalence extends an insight from control theory that establishes a connection between robust and risk-sensitive control. See Hansen and Sargent (2001), Anderson et al. (2003), Hansen and Sargent (2001), and Maenhout (2004) for further elaboration. Special cases of this equivalence first showed up in control theory in the important paper by Jacobson (1973) with many subsequent contributions. With the exception of Hansen and Sargent (1995), however, these papers did not make connections to the recursive utility literature.

iv) *investment productivity*: exogenous shifts in the capital evolution that have persistent consequences.

The first three channels are explicitly linked to climate change and contribute to our analysis in specific ways. We include the fourth channel to provide a benchmark for comparison. By design, it captures the familiar "long-run risk" contributions to the macroeconomy in the absence of climate change.

The uncertainty decompositions that we implement explore intermediate problems with alternative limits on the forms of misspecification.[21] For instance, we will activate each of the four uncertainty channels separately and compare the results with the two benchmarks.[22]

We also consider uncertainty decompositions that activate robustness considerations either prior to the first jump or after the first jump to determine when the impact of the uncertainty is most consequential.

6 State and control variables

In our computations that follow, we use the state variables:

$$X_t \stackrel{\text{def}}{=} \begin{bmatrix} X_t^1 \\ \widehat{N}_t \end{bmatrix} \quad \text{where} \quad X_t^1 \stackrel{\text{def}}{=} \begin{bmatrix} \widehat{K}_t \\ \widehat{R}_t \\ Y_t \end{bmatrix},$$

where

$$\widehat{K}_t \stackrel{\text{def}}{=} \log K_t \quad \widehat{R}_t \stackrel{\text{def}}{=} \log R_t \quad \widehat{N}_t \stackrel{\text{def}}{=} \log N_t.$$

[21] Recently, Cappelli et al. (2021) have explored the source dependence of uncertainty from an abstract decision-theoretic perspective, but without reference to misspecification aversion.

[22] Ricke and Caldeira (2014) implemented a conceptually distinct but similarly motivated approach as displayed in Figure 3 of their paper. Ricke and Caldeira featured three alternative sources of uncertainty that contribute to climate change, where uncertainty is equated to model heterogeneity. Whereas they eliminate the uncertainty from each channel in their decomposition, we close down the *aversion* to uncertainty within a decision-making framework. We also focus on different channels, including damages and technological uncertainty. But we do not look at a more refined decomposition of temperature dynamics as Ricke and Caldeira (2014) do.

We treat the damage jump and technology jump realizations as implying continuation values for the post-jump outcomes. These become inputs into HJB equations prior to the jump. We compute a representation for the continuation values as

$$V(X_t) = \widehat{V}(X_t^1) - \widehat{N}_t\,,$$

where it is straightforward to verify the additive separability in the logarithm of damages. This separability simplifies our numerical solutions. We have three controls:

$$\frac{I_t^k}{K_t}, \quad \frac{I_t^r}{K_t}, \quad \mathcal{E}_t.$$

Consumption is then determined by the output constraint (13). We solve the model using an iterative scheme whereby we iterate between maximization and minimization controls and a finite difference solution for the social value function.

6.1 First-order conditions for maximization

The social planner has two investment opportunities in our model: investment in new capital and investment in R&D. We investigate the first-order conditions prior to the realization of either technology or damage jump. In both cases we see the role of the shadow value of the corresponding asset stock.

The first-order conditions for investment in new capital are

$$\frac{\partial V}{\partial \hat{k}}(X_t)\left(1-\kappa\,\frac{I_t^k}{K_t}\right) - \delta\,\left(\frac{K_t}{C_t}\right) = 0,$$

Thus we obtain the formula for investment:

$$\frac{I_t^k}{K_t} = \frac{1}{\kappa}\left(1 - \frac{\delta K_t}{C_t\left[\frac{\partial V}{\partial \hat{k}}(X_t)\right]}\right),$$

where the term

$$\frac{C_t\left[\frac{\partial V}{\partial \hat{k}}(X_t)\right]}{\delta\, K_t}$$

is the "Q" from the theory of investment. adjusted for damages. In addition to the partial derivative of the value function, this term includes an adjustment for the marginal utility of consumption. The division by K_t occurs because of our choice of $\log K_t$ as a state variable. The damage contribution scales both C_t and K_t and has offsetting impacts on each. The term $\frac{\partial V}{\partial \hat{k}}$ reflects social valuation, which may be distinct from a marginal valuation.

The first-order conditions for the socially efficient R&D investment are

$$\frac{\partial V}{\partial \hat{r}}(X_t)\psi_0\psi_1\left(\frac{I_t^r}{R_t}\right)^{\psi_1-1} - \delta\left(\frac{N_t}{C_t}\right) = 0.$$

Thus

$$\left(\frac{I_t^r}{R_t}\right)^{1-\psi_1} = \psi_0\psi_1\left[\frac{C_t\frac{\partial V}{\partial \hat{r}}(X_t)}{\delta\, N_t}\right].$$

The term in square brackets is the social value of the knowledge stock of R&D expressed in units of (damaged) consumption.

The first-order conditions for emissions are

$$\begin{aligned}&\left[\frac{\partial V}{\partial y}(X_t) - \lambda_1 - \lambda_2 Y_t\right]\left[\bar{\theta} + \varsigma H_t\right] + \mathcal{E}_t\left[\frac{\partial^2 V(X_t)}{\partial y^2} - \lambda_2\right]|\varsigma|^2\\ &+ \delta\,(C_t)^{-1}\,\frac{\phi_0\phi_1}{\beta}\left(\frac{A_t^b}{\beta\alpha K_t}\right)^{\phi_1-1}\mathbf{1}_{\{\mathcal{E}_t<\beta\alpha K_t\}} = 0.\end{aligned}$$

The implied social cost of carbon is

$$\frac{\left[-\frac{\partial \hat{V}}{\partial y}(X_t, Z_t) + \lambda_1 + \lambda_2 Y_t\right]\left(\bar{\theta} + \varsigma H_t\right) - \mathcal{E}_t\left[\frac{\partial^2 V(X_t)}{\partial y^2} - \lambda_2\right]|\varsigma|^2}{\delta\left(\frac{N_t}{C_t}\right)}, \tag{19}$$

and the social benefit is

$$\frac{1}{N_t}\frac{\phi_0\phi_1}{\beta}\left(\frac{A_t^b}{\beta\alpha K_t}\right)^{\phi_1-1}\mathbf{1}_{\{\mathcal{E}_t<\beta\alpha K_t\}},$$

where the formulas are evaluated at the socially efficient allocation inclusive of the misspecification adjustment. Notice also that social cost of carbon (19) includes an explicit volatility adjustment because emissions in our model alter the local exposure to Brownian motion risk.

For all three first-order conditions we see a central role for the partial derivative of the

value function with respect to to an endogenous state, the logarithm of capital, the logarithm of the stock knowledge capital, and temperature.

6.2 Post jump continuation values

There are L possible jump contributions. There are $L-1$ potential damage curve realizations and one technology jump realization. The $L-1$ damage curve realizations are mutually exclusive. At the time of a damage curve jump realization, there is a new state variable, with realization $\tilde{y}$, that is the counterpart to the temperature anomaly. This state variable has the same dynamics as the temperature except it is initialized at $\bar{y}$, independent of the temperature, at the time of the jump. We compute the continuation value allowing for one jump, either a technology jump or a damage curve jump, using the intensity $\mathcal{J}^\ell$. If a technology jump occurs first, temperature remains constant, but there is a possibility of a damage curve realization at some time in the future. This damage curve realization is inconsequential because the temperature anomaly remains constant at point where any incremental curvature has no impact on the damages. Thus we drop the damage curve intensities from the computation. The post technology jump continuation value functions are, therefore, all the same, which simplifies our computations.

7 Illustrative computations

In this section we explore the implications of our analysis for an example economy. We focus exclusively on misspecification aversion for three penalty parameter values, $\xi = .15$, $\xi = .075$, and a baseline of misspecification neutrality $\xi = \infty$. We refer to the higher value of ξ as "less aversion" and the lower value as "more aversion."[23] To appreciate the impact of these settings, we display consequences for distorting probabilities, an approach that is commonly employed for robust Bayesian methods. After inspecting these distortions, we explore implications for social valuation and its consequences for R&D emissions, and climate change. Parameter values that we use for this economy are reported in Appendix A.6.

The calculations convey the following insights from our social planner solution:

[23]For the corresponding risk aversion parameters in a recursive utility specification of preferences, less aversion is $\gamma \approx 7.7$, more aversion is $\gamma \approx 14.3$, and neutrality as $\gamma = 1$.

- Including endogenous R&D is a particularly important tool for the planner when confronting the economic consequences of climate change.
- The impact of *technological uncertainty* dominates those of climate and damage uncertainty.
- R&D investment is substantially more sensitive to uncertainty than are reductions in emissions.

The subsections that follow give graphical characterizations of many of our salient findings.

7.1 Uncertainty-adjusted probability distributions

We consider in turn the implied worst-case probabilities that emerge from our analysis for the four sources of uncertainty: climate, damages, productivity, and technology. These are solutions to the minimization problem, evaluated at solutions to the maximization problem. These are not "best-guess" distributions. Rather they are the "worst-case" distributions subject to penalization that are a vehicle by which the planner constructs robustly optimal courses of action. We report results for two specifications of the penalty parameter: $\xi = .075$ (more aversion) and $\xi = .15$ (less aversion). It is straightforward to run our solution code for other values of ξ. As we noted previously, these could be reinterpreted as recursive utility risk aversion parameters, although we prefer the robustness motivation. While it is hard to interpret directly the magnitudes of ξ, we find it valuable to adopt an approach from robust Bayesian methods by inspecting worst-case probability specifications isolating what probability specifications the robust decision rules are optimal with respect to.

We begin the Brownian motion risk distortion prior to any Poisson jumps. These are captured by changes in the local mean or drift and impact only three of our four channels. We abstract from a Brownian contribution to damages. We report these as conditional mean changes in a multivariate standard normal distribution. The results are reported in Table 1 for each of the three endogenous state variables. The computed "worst-case" drift distortions are modest, since the Brownian increments are standardized. With a sign change for capital and the stock of knowledge, these translate into instantaneous uncertainty compensations for social valuation. The most notable one is for the shock to the capital stock, where with

"more aversion" this is a mean compensation of .12 for a standardized normal shock, and for "less aversion" this compensation is only .06. The adjustments for the two other shocks distributions are much smaller and not noteworthy.

Drift distortion for the endogenous state variables			
uncertainty	capital	temperature	knowledge stock
more aversion	-.122	.027	-.006
less aversion	-.063	.008	-.002

Table 1: Conditional mean distortions to Brownian increments for the productive capital, K_t, the temperature anomaly, Y_t, and knowledge capital, R_t. The table reports numbers both under more aversion ($\xi = .075$) and less aversion ($\xi = .15$) to potential model misspecification. The conditional mean shifts are calculated in the initial period.

From Figures 4 and 5 we see that uncertainty aversion distorts the probability distributions used by the planner for the climate and damage models away from the low values and toward the higher values of θ and λ_3. The effect is much more modest for the climate models than the damage models and, as expected, is more pronounced as the aversion is increased (as the penalty parameter, ξ is decreased.)

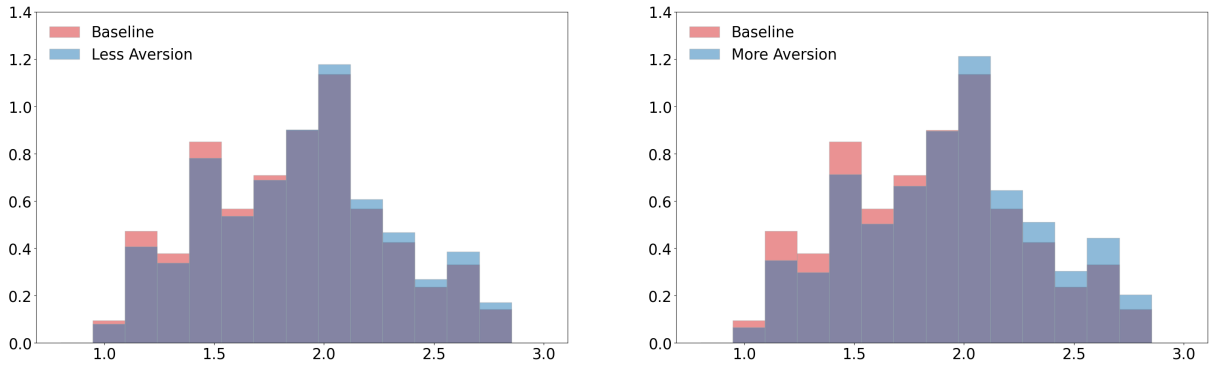

(A) Less Aversion (B) More Aversion

Figure 4: Distorted climate model distribution. The left plot shows the undistorted and distorted distributions with less misspecification aversion. The right plot shows the undistorted and distorted distributions with more misspecification aversion. The histograms are calculated at year 0, with the trajectories leading up to year 0 simulated under the baseline probabilities and abstracting from the intrinsic randomness. Recall that Brownian motion misspecification aversion induces a shift in the local mean. The distorted histograms were constructed by imposing instead ambiguity aversion where the ambiguity penalization was set to capture the same unfavorable conditional mean distortion as the misspecification aversion. See Appendix A.5 for details. The "no aversion" mean of this distribution is 1.86; with less aversion it is 1.91, and with more aversion it is 1.94.

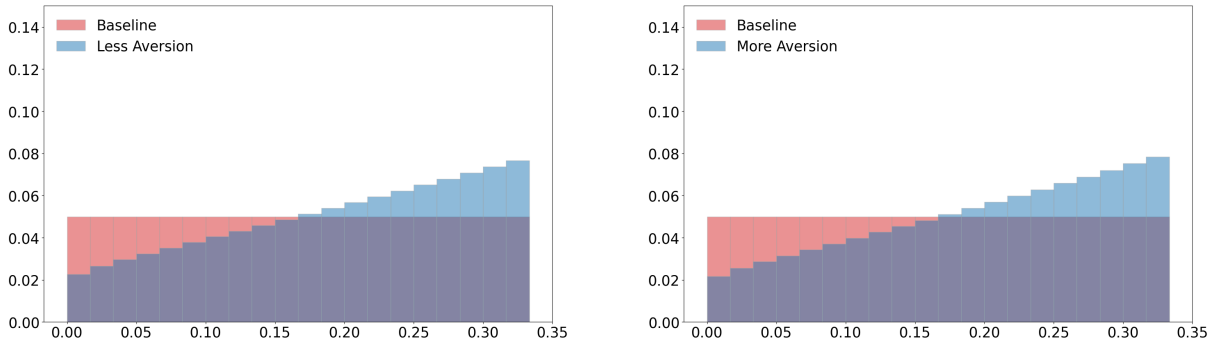

(A) Less Aversion (B) More Aversion

Figure 5: Distorted damage model distribution. The plot shows the undistorted and distorted distributions with less misspecification aversion in the left panel and more misspecification aversion in the right panel. The histograms are calculated at year 0, with the trajectories leading up to year 0 simulated under the baseline dynamics abstracting from the intrinsic randomness.

We next explore densities pertinent to the first jump, which could be any of the L possibilities. We first compute the probability that there has been no jump event prior to time t for each t. This is given by:

$$\widetilde{Prob}(t;x) = \widetilde{E}\left[\exp\left(-\int_0^t \left[\sum_{\ell=1}^{L} \mathcal{J}^{\ell}(X_u) g^{\ell *}(X_u)\right] du\right) \mid X_0 = x\right].$$

The expectation, $\widetilde{E}$, includes the drift distortions. The function, $\widetilde{Prob}(t;x)$ starts at one when $t = 0$, decreases as a function of the horizon t, and converges to zero, as we expect there will eventually be a jump of some kind. Thus $1 - Prob(t;x)$ behaves as a cumulative distribution function of the horizon t with a density given by its derivative with respect to t:

$$\widetilde{prob}(t;x) = -\frac{d}{dt}\widetilde{Prob}(t;x).$$

This resulting density informs us as to the perceived timing of the first jump.

The density for the first jump will depend on the presumed aversion to uncertainty not only through the $g^{\ell *}$'s but also on the expectation used in computing $Prob(t;x)$. We plot the four densities in Figure 6 for the four different configurations of uncertainty aversion. Notice that in all four cases the densities peak around thirty years. By imposing pre-jump uncertainty aversion, the initial (worst-case) probabilities are lower than the uncertainty neutrality counterparts. Since the densities integrate to unity, this initial reduction is offset by higher density modes. These densities are very similar with or without post jump uncertainty aversion. In summary, the more pessimistic outlook for technology captured by the worst-case probabilities have initial reductions in the success probabilities but have modes in the success densities at about the same location as the uncertainty neutral specifications.

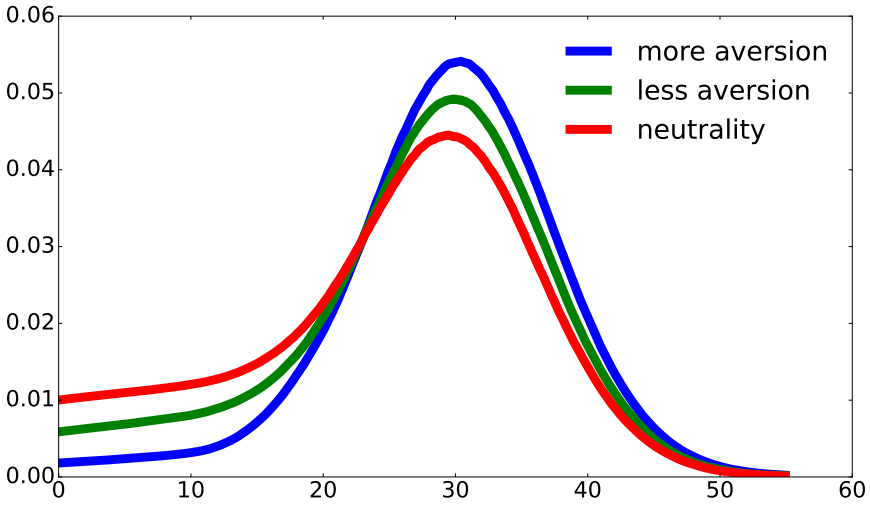

Figure 6: This figure gives three densities $\widetilde{prob}(t;x)$ depending on the value of ξ. In particular, the density labeled "neutrality" ($\xi = \infty$) depicts the baseline probability density specification.

We also compute the following two components featuring either damage or technology jumps separately. The two components add up to the $\widetilde{p}rob$ densities.

$$\widetilde{prob}_1(t;x) = E\left[\exp\left(-\int_0^t \left[\sum_{\ell=1}^{L} \mathcal{J}^{\ell}(X_u) g^{\ell *}(X_u)\right] du\right)\left(\sum_{\ell=1}^{L-1} \mathcal{J}^{\ell}(X_t) g^{\ell *}(X_t)\right) \mid X_0 = x\right]$$

$$\widetilde{prob}_2(t;x) = E\left[\exp\left(-\int_0^t \left[\sum_{\ell=1}^{L} \mathcal{J}^{\ell}(X_u) g^{\ell *}(X_u)\right] du\right)\left(\mathcal{J}^{L}(X_u) g^{L *}(X_u)\right) \mid X_0 = x\right]$$

We see that from Figure 7 that initially a technology jump might occur, but that by year 25 the probability of a damage jump becomes prominent and the more likely first jump. Overall, a damage jump is more likely than a technology jump, but both are quite possible, as is documented in Table 2. The uncertainty-adjusted probabilities give substantially more prominent weight to the damage jump.

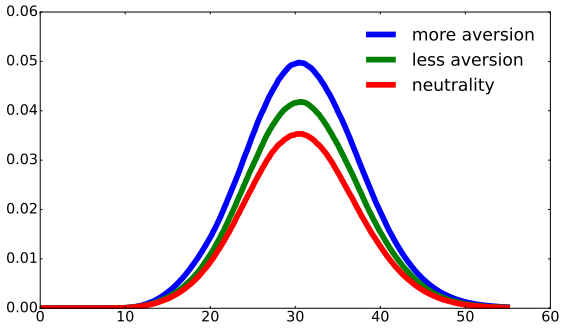

(A) $\widetilde{prob}_1(t;x)$

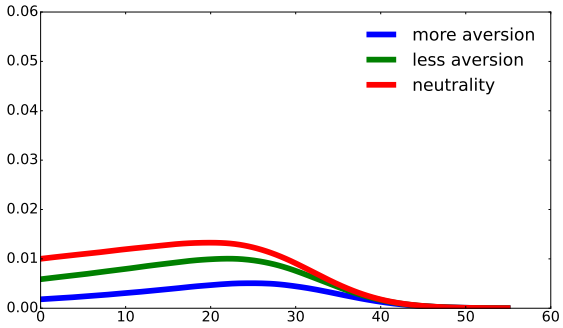

(B) $\widetilde{prob}_2(t;x)$

Figure 7: This figure plots the two components of the $\widetilde{prob}$ densities. The $\widetilde{prob}_1$ components measure the contribution of damage jumps, and the $\widetilde{prob}_2$ components measure the contribution of technology jumps.

ξ	damage jump	technology jump
∞	0.58	0.42
0.15	0.69	0.31
0.075	0.85	0.15

Table 2: This table gives the integrals of the two component curves $\widetilde{prob}_1$ and $\widetilde{prob}_2$.

7.2 Uncertainty impacts on social valuations

We initially consider the impact of uncertainty on the social value of R&D and the social cost of climate change both measured using partial derivatives of the functions. Since temperature changes are harmful we report the negative of the partial derivative. Table 3 gives the uncertainty decompositions for both these social valuations decomposed by the channel to which the uncertainty operates. We report differences in logarithms when all of the channels are activated relative to when each one is activated separately. For both of the social valuations, the technological uncertainty accounts for the bulk of the uncertainty enhancement. For instance, there is only a 6% reduction in the social value of R&D and a 9%

reduction in the social cost of global warming when only the technology uncertainty channel is activated.[24]

Uncertainty channel	$\Delta \log \text{SVRD}$		$\Delta \log \text{SCGW}$	
	$\xi = 0.15$	$\xi = 0.075$	$\xi = 0.15$	$\xi = 0.075$
climate uncertainty	0.31	0.61	0.45	0.97
damage uncertainty	0.30	0.60	0.43	0.93
productivity uncertainty	0.33	0.67	0.48	1.02
technology uncertainty	0.06	0.15	0.09	0.24

Table 3: Uncertainty decompositions for social valuations for the four different channels of uncertainty. The table entries in the first four rows are the difference between the logarithms of the values or costs when all four channels are activated minus the logarithms for each of the different channels. The table entries in the last row are the difference in logarithms of value or costs when all four channels are activated minus the logarithm when none of the channels are activated. The numbers are for the initial time period.

7.3 Robust actions

This subsection explores implications for robustly optimal actions. Actions and values are closely tied via first-order conditions, but it remains revealing to show the outcomes for both R&D and emissions. We explore expected trajectories demonstrating the mean of simulated outcomes averaging across random realizations of the Brownian shocks and the Poisson jumps. We refer to these pathways as "expected" pathways. We also report a small set of stochastic trajectories illustrating some of the different realizations of the Poisson events. Both sets of trajectories are simulated under baseline probabilities.

7.3.1 Expected trajectories

We first examine the expected trajectories. We report pathways up to year thirty. From Figure 6 we know that these expected trajectories necessarily incorporate realizations for technological innovation and damage function curvature jumps.

[24]The contributions are not constructed to be additive.

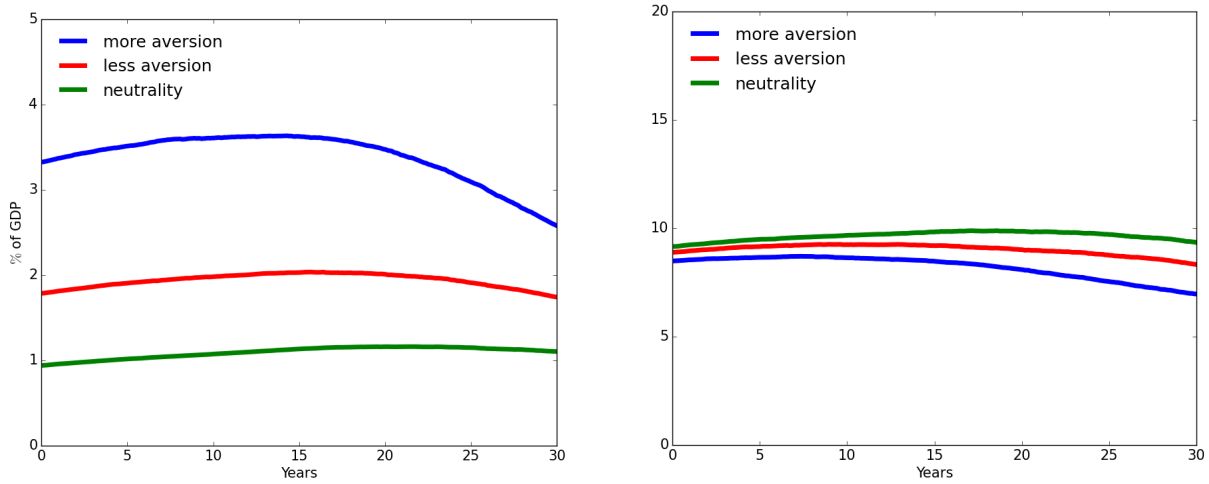

(A) R&D investment

(B) Emissions

Figure 8: Simulated expected pathways of R&D investment as a fraction of output and emissions in gigatons of carbon (GtC). Panel A compares outcomes of R&D investment for different values of the misspecification aversion parameter ξ. Panel B compares outcomes of emissions for different values of the misspecification aversion parameter ξ. The trajectories are simulated under the baseline transition dynamics averaging over Brownian and jump shocks.

Panel A of Figure 8 gives the expected pathways for the robustly optimal choice of R&D investment (Panel A) and emissions (Panel B) for different values of uncertainty aversion (neutrality in green, less aversion in red, more aversion in blue). While there is considerable investment in R&D chosen by the planner, Panel A shows a substantial increase in this investment in the presence of misspecification aversion. Even with the more modest specification of this aversion ($\xi = 0.15$), the investment is almost doubled relative to that of the neutrality specification ($\xi = \infty$). With uncertainty aversion, the R&D investment pathways increase initially and then gradually decline over time as the technological innovation becomes more likely to be realized.

Panel B shows that while emissions are reduced when the fictitious planner is more concerned about potential model misspecification, the uncertainty impact is quite muted, at least initially. Eventually, the emissions then modestly taper off over time, with the decline more pronounced the greater is the uncertainty aversion. This taper is impacted by damage curve realizations for more extreme temperature changes. The fictitious planner

sets emissions in hopes of delaying the potential realization of more extreme damages so that R&D has a greater chance of being successful. This incentive is partially offset by the need for energy as an input into production of output. Sizable reductions in output not only has ramifications for consumption, but also for both types of investment.

The increase in R&D investment as misspecification aversion increases is particularly striking. The planner reduces the investment-output ratio to offset the increase in R&D investment. Since R&D investment is much smaller than investment in the productive stock, the proportional reduction in the latter investment is much smaller. As we documented in Table 3, uncertainty about the R&D technology is of particular concern to the planner. For this reason, the R&D investment increase might not seem surprising. In addition, the enhancement in R&D investment accelerates the prospects of successful discovery and reducing the future exposure to uncertainty. In Section 8, we decompose the forces influencing the robustly optimal choice for investment in R&D to highlight the underlying mechanisms driving the responses to uncertainty concerns.

To push this analysis further, we verified numerically that a sufficiently large increase in the aversion to misspecification uncertainty (a sufficiently small reduction in ξ) reduces the R&D investment-output to essentially zero with implied worst-case probabilities that make a discovery very unlikely for the relevant decision-making horizons of our planner. Thus the impact of the degree of uncertainty aversion on R&D investment is not monotonic. It increases, however, over a range that we find to be interesting and plausible. Further details and figures are provided in Appendix D.1.

7.3.2 Stochastic trajectories

We now examine five stochastic trajectories illustrating some of the different realizations of the Poisson events:

i) no jumps for forty years;

ii) damage jump at year 28 is accompanied by a low damage curve realization;

iii) damage jump at year 36 is accompanied by a high damage curve realization;

iv) technology jump to a clean technology at year 26;

v) technology jump to a clean technology at year 20.

These simulated pathways allow for random realizations of the Brownian and Poisson shocks, and are derived from the same model solutions that are used to produce the expected pathways above. The reported paths were computed under the preference specification with less aversion. We refer to these pathways as "stochastic" pathways.

Figure 9 gives the stochastic pathways for optimal choice of R&D investment (Panel A) and emissions (Panel B) for these different stochastic realizations under the less aversion setting. Panel A illustrates some of the impacts of the Poisson events on the R&D investment trajectories. Each case begins with substantial R&D investment. When the technology jump occurs (Paths 4 and 5), R&D investment drops to zero, showing how the planner does not expect elevated levels of R&D indefinitely. However, when the damage jump occurs first, R&D investment can either jump down for a good realization of the damage curvature λ_3 (Path 2) or jump up for a bad realization of λ_3 (Path 3). Otherwise the R&D investment remains persistent without one of these jumps occurring (Path 1). Panel B shows the dramatic impact of the technology discovery on emissions, allowing for emissions to drop to zero along trajectories with technological innovation shocks (Paths 4 and 5), including one that happens in year twenty (Path 5). In addition, when a damage jump occurs before the technology jump, the path of emissions can shift down for a bad realization of λ_3 (Path 3), or possibly stay the same or even increase for a relatively good λ_3 realization (Path 2). Again without a jump (Path 1), the emissions pathway is persistent.

We conclude this subsection by looking at the consequences for temperature along the illustrative stochastic trajectories as reported in Panel C of Figure 9. Notice that in the next forty years only one of the trajectories (Path 2, good λ_3 realization) approaches a two degree anomaly for a prudent social planner with modest misspecification aversion. The scenarios with technology jumps (Paths 4 and 5) halt temperature increase at $1.5^{\circ}C$ and $1.8^{\circ}C$, respectively, whereas the case with a bad λ_3 realization (Path 3) and no jumps (Path 1) have increasing temperature anomalies that stay below two degrees. This highlights that relatively cautious emissions pathways are chosen to try to avoid the most severe climate change consequences.

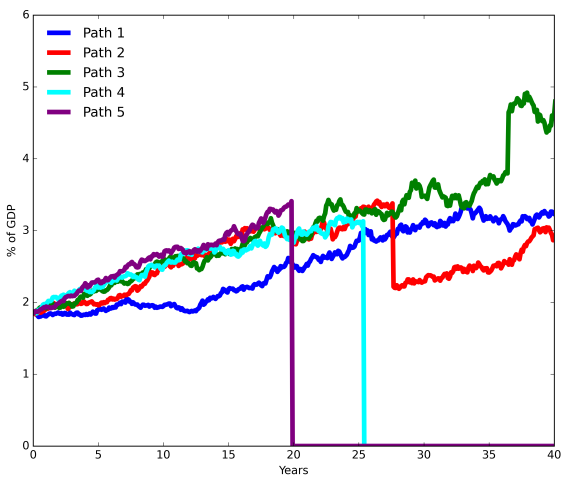

(A) Stochastic Simulation Pathways: I_t^r

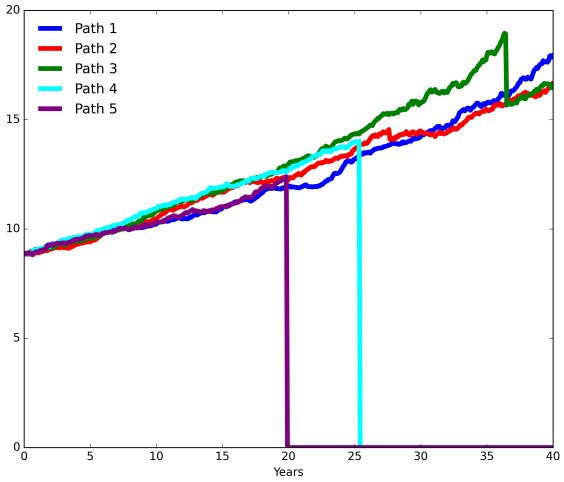

(B) Stochastic Simulation Pathways: $\mathcal{E}_t$

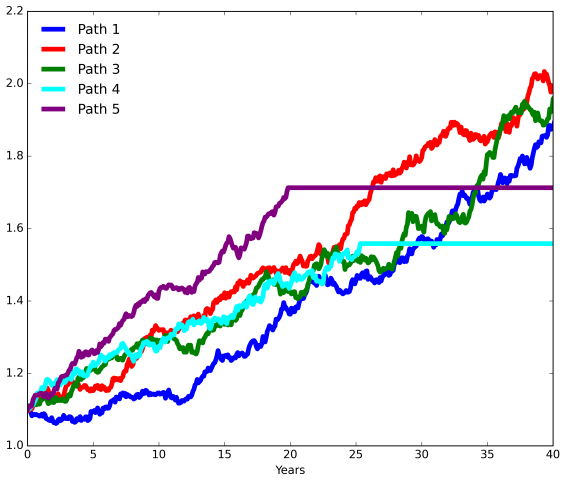

(C) Stochastic Simulation Pathways: $\hat{Y}_t$

Figure 9: Simulated stochastic pathways for emissions and R&D investment as a fraction of output, emissions, and temperature. Panel A shows pathways of R&D investment for the five illustrative stochastic scenarios. Panel B shows pathways of emissions for the five illustrative stochastic scenarios. Panel C shows corresponding pathways of temperature for the five illustrative stochastic scenarios temperature. The trajectories are simulated under the baseline transition dynamics with less uncertainty aversion.

8 Isolating alternative forces for investment in R&D

The R&D investment is initially fifty percent higher under the more modest specification of uncertainty aversion relative to uncertainty neutrality. This is an example of where enhanced concerns about uncertainty makes the planner more proactive. There are two competing forces in play that underlie this outcome. On the one hand, the planner is more skeptical of timing of when the new fully clean technology will replace energy that generates fossil fuel emissions. This makes the investment less attractive. On the other hand, the rewards to an R&D success are enhanced, making the investment more attractive. We use value decompositions derived in Section 3 building on insights from asset pricing theory. For pedagogical simplicity we focus on the case in which the only source of uncertainty is in the R&D dynamics, which showed to be the dominant concern. The appendix reports the corresponding results when uncertainty is activated in all four channels.

8.1 Value Decomposition

We interpret the partial derivative of the value function with respect to the R&D knowledge state as an asset price. As such it has four payoff contributions as we have derived previously:

i) $\delta m \cdot \frac{\partial U}{\partial x}$;

ii) $m \cdot \sum_{\ell=1}^{L} \frac{\partial \mathcal{J}^\ell}{\partial x}(V^\ell - V)$;

iii) $m \cdot \sum_{\ell=1}^{L} \mathcal{J}^\ell \frac{\partial V^\ell}{\partial x}$

iv) $\xi m \cdot \sum_{\ell=1}^{L} \frac{\partial \mathcal{J}^\ell}{\partial x}(1 - g_\ell^* + g_\ell^* \log g_\ell^*)$.

Terms ii) and iv) simplify further because $\frac{\partial \mathcal{J}^\ell}{\partial r} = 0$ except for $\ell = L$, which is the technology jump. Term iii) has a *direct* contribution coming from

$$\sum_{\ell=1}^{L-1} \mathcal{J}^\ell \frac{\partial V^\ell}{\partial \hat{r}}.$$

Note that the continuation value function V^L does not depend on the R&D stock because it conditions on the R&D success. Term iii) also has indirect contributions because marginal

change in the initial stock of R&D also induces marginal changes in the other state variables. While the continuation values V^{ℓ} for $\ell = 1, 2, ..., L-1$ do not depend on the pre-jump temperature, term iii) includes contributions from the damage jumps as these will depend on the knowledge stock along with the other state variables. Term iv) reflects the reduction in the uncertainty challenges associated with a technology jump. These four contributions to the marginal values add up to the total. In computations that follow, we measure them separately. In addition, we will split the contribution to iii) coming from the damage curve realization jumps ($\ell = 1, ..., L-1$) and the technology discovery jump ($\ell = L$).

We also consider four different configurations of uncertainty aversion as a way to assess the different economic forces in play:

a) pre-jump neutrality - post-jump neutrality;

b) pre-jump neutrality - post-jump aversion

c) pre-jump aversion - post-jump neutrality

d) pre-jump aversion - post-jump aversion

We include cases b) and c) because they provide revealing intermediate cases that help understand the overall uncertainty implications. For instance, there are two forces in play. First, uncertainty about when the new technology will become realized would seem to make investment in R&D less attractive. Second, the positive implications for a technological success can be stronger when there is more aversion to this uncertainty. Intermediate case c) allows us to feature more the first force, while intermediate case b) shifts the attention to the second force. With these intermediate cases, we can better assess the quantitative magnitude of these offsetting forces.

The results are reported in Table 4.

case	i	ii	iii(dc)	iii(td)	iv	sum
pre neutrality						
a) post neutrality	0.0019	0.0129	0.0136	0.0017	0.0000	0.0300
b) post aversion	0.0026	0.0161	0.0157	0.0026	0.0000	0.0370
pre aversion						
c) post neutrality	0.0019	0.0096	0.0160	0.0012	0.0024	0.0311
d) post aversion	0.0027	0.0110	0.0200	0.0018	0.0039	0.0396

Table 4: Components to the partial derivative of the value function with respect to the R&D state variable. The column iii(dc) includes only the contributions from the damage curve realization jumps to iii, and iii(td) includes the remaining contribution from the technology discovery jump to iii.

The partial derivative decomposition in Table 4 reveals the following;

- the totals for pre aversion-post aversion (0.040) are very close to pre neutrality post aversion (0.037);
- the continuation value contributions ii) and iii) are larger for pre neutrality-post aversion than they are for pre neutrality-post neutrality as might be expected;
- the continuation value contribution iii) is primarily due to the damage jumps and not to the technology jump;
- the total for pre aversion-post neutrality (.031) is only slightly larger than the total for pre neutrality-post neutrality (.030). The difference is more than offset by the relative entropy contribution to the pre neutrality - post aversion total.

In terms of the fourth observation, when we net out the entropy contribution, the pre-jump uncertainty contribution reduces the marginal valuation because of the more pessimistic view of the success of R&D. This reduction turns out to be quite small, however. Perhaps this small magnitude should be anticipated because of our very low subjective discount rate. For instance, by driving the discount rate to zero, we make the timing of the success less relevant in the decision making.

8.2 Expected marginal social payoffs for alternative horizons

As we demonstrated, the derivative of the value function has the interpretation as a stochastically discounted social cash flow with the four contributions given at the outset of Section 8.1. The "stochastic discount factor" includes the vector of stochastic impulse responses, the process M, along with the subjective rate of discount, δ. Figure 10 shows the period-by-period contribution for each of the four components.

Both of the continuation value contributions to the social cash flow, terms ii) and iii), are important contributors to the marginal value of R&D, but there is rather substantial differences in their horizon dependence. Term ii) has an important initial contribution that then gradually vanishes so that by a thirty year horizon it is between one fourth and a third of its initial impact, depending on the uncertainty configuration. In contrast, term iii) is initially very small but has a substantial peak effect by year thirty. Both contributions are enhanced by post jump uncertainty aversion. Its impact on marginal valuation remains important well past a horizon of forty years, reflecting the long-term nature of the valuation. The direct marginal utility contribution, term i), is small across all horizons, although it does increase up to twenty years. The entropy contribution, term iv), is also relatively minor across all horizons and uncertainty aversion configurations, though the initial magnitude is augmented by pre jump uncertainty aversion and this effect persists out to thirty years.

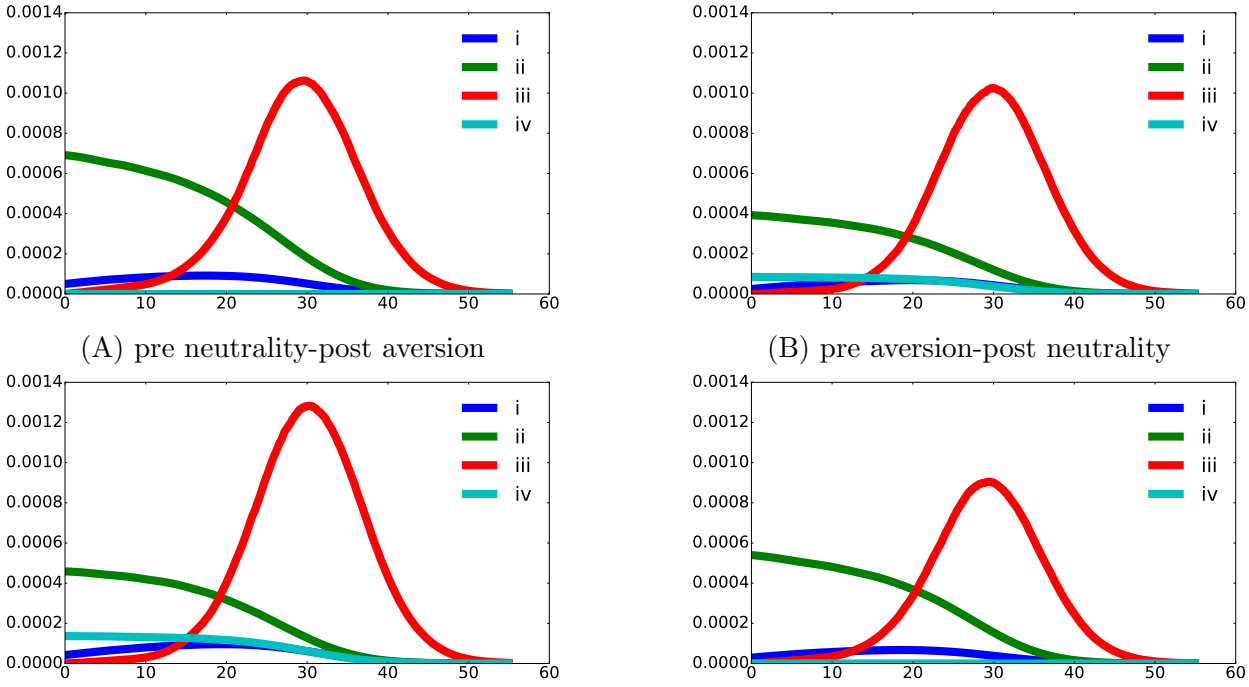

(A) pre neutrality-post aversion

(B) pre aversion-post neutrality

(C) pre aversion-post aversion

(D) pre neutrality-post neutrality

Figure 10: Horizon decomposition of social cash flow contributions to the R&D stock valuation. The four panels correspond to different uncertainty aversion configurations: Panel A is the pre neutrality-post aversion configuration; Panel B is the pre aversion-post neutrality configuration; Panel C is the pre aversion-post aversion configuration; and Panel D is the pre neutrality-post neutrality configuration. The blue lines correspond to the payoff contribution i) $\delta m \cdot \frac{\partial U}{\partial r}$. The green lines correspond to the payoff contribution ii) $m \cdot \sum_\ell \frac{\partial \mathcal{J}^\ell}{\partial r}(V^\ell - V)$. The red lines correspond to the payoff contribution iii) $m \cdot \sum_\ell \mathcal{J}^\ell \frac{\partial V^\ell}{\partial r}$. The light blue lines correspond to the payoff contribution iv) $\xi m \cdot \sum_\ell \frac{\partial \mathcal{J}^\ell}{\partial r}(1 - g_\ell^* + g_\ell^* \log g_\ell^*)$.

In summary, the more skeptical assessment of R&D prospects prior to a jump induce only a quantitatively minor adverse impact on the incentive for R&D investment. A possible R&D success, however, gives a quantitatively important incentive for more R&D investment. While these quantitative results are special and tied to our model calibration, these competing forces are likely to be in play in more general circumstances.

Remark 8.1. *Recall that this is "big project" R&D analogous perhaps to the Manhattan project or the Apollo program with uncertainty in the R&D investment only about the timing of a successful outcome or social payoff. For the reasons we have exposited, more R&D*

leads to an increased likelihood that the new, clean technology will be discovered sooner even though the uncertainty in the technology may be greater. This increase in a more uncertain investment stands in contrast to a standard portfolio allocation problem with riskless and uncertainty investment alternatives. In this latter problem, an enhanced concern about uncertainty leads to a reduction in the portfolio weight associated with the uncertain investment.

9 Model Sensitivity

In preceding sections we have featured the sensitivity of social valuation and policy outcomes to changes in the aversion to misspecification, aversion that is reflected in implied uncertainty-adjusted probability distributions. We now briefly discuss sensitivity to changing the subjective rate of discount (δ) and changing the intertemporal elasticity of substitution (IES) (ρ). Further details are provided in Appendices D.2 - D.3.

The prior environmental economics literature has explored sensitivity of the SCC to changes in the "discount rate." Often these analyses feature the implied discount rate used in computing present values abstracting from stochastic discounting. In our setting with misspecification, stochastic discounting is a central ingredient in valuation, as is expected from our understanding of asset pricing. In particular, we have featured how uncertainty aversion preferences impact an endogenously determined change in the probability measure that is pertinent for valuation. Increasing δ from .01 to .015, we see drops in the valuations by about 30%, confirming a sensitivity often noted in the environmental economics literature.

We also consider two alternative specifications of the IES: $\rho = 2/3$ and $\rho = 3/2$ using the preferences defined in Appendix A.4. Much of the asset pricing literature has studied the consequences of changing the IES on asset valuation within the setting of an endowment economy. Our economy is a production economy, however, and changing the IES has a big impact on production outcomes. As expected from growth models, the investment in both types of capital relative to output are higher when the elasticity is greater (ρ is smaller). R&D investment is more than doubled initially when we increase the IES to 3/2, with just the opposite effect when we decrease the IES to 2/3. The valuations of the corresponding capital stocks move in the opposite way, as expected. The implied emissions trajectories for the two alternative specifications of the IES show some modest differences at the outset and marked differences in the slope of the trajectories, with lower values for the case of $\rho = 2/3$

as compared to the case of $\rho = 3/2$. The growth sensitivities in emissions prior to any jumps are consistent with the investment differences, since higher investment helps support more initial growth in output.[25]

10 Conclusions

We propose and implement methods for assessing the consequences of uncertainty on social values and prudent courses of action. We show how to use the policy problem to assess the relative importance of the alternative channels by which uncertainty can alter decisions, policies and outcomes. We also derive an asset pricing representation for social valuations associated with the endogenous state variable in the underlying dynamical system. We show how these representations are altered by misspecification aversion and how to use them to assess important contributors to social valuation. There are straightforward extensions of these methods to i) accommodate versions of so-called "smooth ambiguity aversion" represented as explorations of prior/posterior sensitivity, and ii) to assess the the marginal impact of *ad hoc* policies that may fail to achieve full optimality in the presence of robustness concerns.

Our substantive findings emphasize the potential importance of including endogenous R&D investment into quantitative assessments of socially prudent courses of action along with current and near-term future carbon reductions. Our calculations expose the limitations of commonly proposed policy solutions that entail a gradual decrease of emissions to a net zero target. Further research is needed to explore robustness of such gradualist approaches to confronting the threat of climate change. In addition, R&D provides our fictitious social planner with a second investment opportunity. More uncertainty in the payoff to this investment can result in an increase in the R&D investment relative to output needed to accelerate the possible discovery of a new economically viable green technology. This provides a substantively important example when *more aversion* to potential model misspecification leads to *bolder actions* on the part of the decision maker.

[25]When discussing our paper, Eric Renault reminded us that there can be seemingly counterintuitive interactions between the IES and the risk aversion in recursive utility models, noting that the latter is not a "pure" risk aversion parameter. Indeed, in dynamic stochastic settings, the intertemporal composition of risk comes into play when exploring the preference implications. See Cai and Lontzek (2019) and Hambel et al. (2021) for related discussions when exploring the SCC. The changing implications for consumption and investment induced by changes in the IES make the risk aversion comparisons all the more tricky.

We end by giving our opinionated and speculative discussions of more pragmatic policy challenges. A common objection to taking strong immediate action on climate change by skeptics who accept the climate science behind global warming is that the costs of using inefficient government approaches to confront the problem undermine attractiveness of public as opposed to market solutions. A blunt way of putting this objection is, "This problem won't be solved by government throwing money at it." While there are good reasons to be skeptical about political processes undermining the attractiveness of collective action, our robustness calculations suggest that the uncertainties, broadly conceived, may be large enough to push for efforts to overcome political distortions and embark on investment directed to the discovery of economically viable clean alternatives. What is missing in our analysis is a more serious probe into the political economy of large-scale public investment projects. Nevertheless, our formulation and robustness analysis feature the potential for stimulating R&D investment in truly novel technologies rather than through subsidies that create inefficiencies and special interest rent seeking.

A Appendix

Below we provide the details and derivations for various results in the main text. As in the main text, throughout the appendix we let lower-case variables capture potential realizations of random vectors. Additional plots and figures can be found in our online notebook:

A.1 Climate model uncertainty

We construct 144 different TCRE's by using 100 GtC pulse experiment results of Joos et al. (2013) tracing out the resulting carbon in the atmosphere for 9 different models. We then use these as inputs into 16 model approximations for temperature responses using the approximation in Geoffroy et al. (2013) to build the collection of θ_ℓ's used in our analysis.

A.2 Damage function

The solution to the differential equation (16) is

$$\hat{n}(y) = \begin{cases} \lambda_1 y + \frac{\lambda_2}{2} y^2 & y \leqslant \tilde{y} \\ \lambda_1 y + \frac{\lambda_2}{2}(\bar{y} + y - \tilde{y})^2 + \frac{\lambda_3(z_n)}{2}(y - \tilde{y})^2 - \frac{\lambda_2}{2}(\bar{y})^2 + \frac{\lambda_2}{2}\tilde{y}^2 & \tilde{y} < y, \end{cases}$$

or equivalently

$$\hat{n}(y) = \begin{cases} \lambda_1 y + \frac{\lambda_2}{2} y^2 & y \leqslant \tilde{y} \\ \lambda_1 y + \lambda_2 \bar{y}(y - \tilde{y}) + \frac{\lambda_2 + \lambda_3(z_n)}{2}(y - \tilde{y})^2 + \frac{\lambda_2}{2}\tilde{y}^2 & \tilde{y} < y. \end{cases}$$

A.3 Production function interpretation of abatement

We verify that the first derivatives are positive and that the second-derivative matrix is negative semi-definite when we interpret

$$\alpha k \left(1 - \phi_0(z) \left(\iota\right)^{\phi_1}\right)$$

for

$$\iota = \left(1 - \frac{e}{\beta \alpha k}\right) \mathbf{1}_{\{0 \leqslant e \leqslant \beta \alpha k\}}$$

as a production function.[26] Notice that the candidate production function is homogeneous of degree one in (e, k).

First, we consider the partial derivatives with respect to e:

$$\begin{aligned}
\frac{\partial}{\partial e}\text{output} &= \alpha k\, \phi_0(z)\, \phi_1\, (\iota)^{\phi_1 - 1}\, \frac{1}{\beta \alpha k} \\
&= \frac{\phi_0(z)\, \phi_1}{\beta}\, (\iota)^{\phi_1 - 1} \\
&> 0 \\
\frac{\partial^2}{\partial e^2}\text{output} &= -\frac{\phi_0(z)\phi_1(\phi_1 - 1)}{\beta^2 \alpha k}\, (\iota)^{\phi_1 - 2} \\
&< 0.
\end{aligned}$$

If $\phi_1 > 2$, both derivatives are zero at $e = \beta \alpha k$. This remains true for $e > \beta \alpha k$.

Next we consider derivatives with respect to k:

$$\begin{aligned}
\frac{\partial}{\partial k}\text{output} &= \alpha \left(1 - \phi_0(z)\, (\iota)^{\phi_1}\right) - \phi_1 \phi_0(z) \alpha k\, (\iota)^{\phi_1 - 1} \left(\frac{e}{\beta \alpha k^2}\right) \\
&= \alpha \left(1 - \phi_0(z)\, (\iota)^{\phi_1}\right) - \phi_1 \phi_0(z)\, (\iota)^{\phi_1 - 1} \left(\frac{e}{\beta k}\right) \\
\frac{\partial^2}{\partial k^2}\text{output} &= -\frac{\phi_0(z)\phi_1(\phi_1 - 1)}{\beta^2 \alpha k}\, (\iota)^{\phi_1 - 2} \left(\frac{e}{k}\right)^2 \\
&< 0.
\end{aligned}$$

The first derivative is $\alpha(1 - \phi_0) \geqslant 0$ when $k \to \infty$ and $\alpha > 0$ when $\beta \alpha k \leqslant e$. Given the negative second derivative, the first derivative remains positive for $k > 0$.

The simple relationship between the second derivatives with respect to e and k is to be anticipated, since the first derivatives are homogeneous of degree zero. Consistent with this relationship, the cross partial is

$$\frac{\partial^2}{\partial e \partial k}\text{output} = \frac{\phi_0(z)\, \phi_1(\phi_1 - 1)}{\beta^2 \alpha k}\, (\iota)^{\phi_1 - 2} \left(\frac{e}{k}\right).$$

[26] For notational simplicity, we drop the dependence of ϕ_0 on z.

The negative semi-definite Hessian matrix follows since

$$\begin{aligned}\begin{bmatrix}\mathsf{r}_1 & \mathsf{r}_2\end{bmatrix}\begin{bmatrix}\frac{\partial^2}{\partial e^2}\text{output} & \frac{\partial^2}{\partial e\partial k}\text{output}\\ \frac{\partial^2}{\partial e\partial k}\text{output} & \frac{\partial^2}{\partial k^2}\text{output}\end{bmatrix}\begin{bmatrix}\mathsf{r}_1\\ \mathsf{r}_2\end{bmatrix} &= \frac{\partial^2}{\partial e^2}\text{output}\begin{bmatrix}\mathsf{r}_1 & \mathsf{r}_2\end{bmatrix}\begin{bmatrix}1 & -\frac{e}{k}\\ -\frac{e}{k} & \left(\frac{e}{k}\right)^2\end{bmatrix}\begin{bmatrix}\mathsf{r}_1\\ \mathsf{r}_2\end{bmatrix}\\ &= \frac{\partial^2}{\partial e^2}\text{output}\left(\mathsf{r}_1-\mathsf{r}_2\frac{e}{k}\right)^2\\ &\leqslant 0.\end{aligned}$$

A.4 Social planner preferences IES values different than unity

We adopt a recursive representation of preferences in continuous time for the planner extended to allow for $\rho > 1$. We start by forming the continuation value for each calendar date as follows:

$$\exp(V_t) = \left(\delta\int_0^\infty \exp(-\delta\tau)\left(C_{t+\tau}\right)^{1-\rho}d\tau\right)^{\frac{1}{1-\rho}}$$

where $\exp(V)$ gives an ordinally equivalent representation of preferences since $\exp(\cdot)$ is an increasing function. These preferences are dynamically consistent with a recursive representation.[27]

The following differential equation gives the local representation:

$$\lim_{\epsilon\downarrow 0}\frac{1}{\epsilon}\left(V_{t+\epsilon}-V_t\right) = -\frac{\delta}{1-\rho}\left[\left(\frac{(C_t)^{1-\rho}}{\exp\left[(1-\rho)V_t\right]}\right)^{1-\rho}-1\right] \tag{20}$$

which is a backward recursion linking future continuation values to the current one. Introducing stochasticity under a risk specification and rearranging terms gives:

$$0 = \frac{\delta}{1-\rho}\left[\left(\frac{(C_t)^{1-\rho}}{\exp\left[(1-\rho)V_t\right]}\right)^{1-\rho}-1\right] + \lim_{\epsilon\downarrow 0}\frac{1}{\epsilon}\left[\mathbb{E}\left(V_{t+\epsilon}\mid\mathfrak{F}_t\right)-V_t\right].$$

As in case when $\rho = 1$, we use the robustness adjustments derived in Section 2 to replace local mean of the continuation value implied by the candidate value function.

[27] This consistency is evident by raising both sides of the equation V_t to the power $1-\rho$ and scaling by $\frac{1}{1-\rho}$ to make the transformation increasing.

A.5 Incorporating ambiguity aversion

Imagine there are alternative models of different components of the dynamics. We follow Hansen and Miao (2018) by supposing that the drift $\mu(x, a \mid \theta)$ depends on an unknown parameter θ residing in a set Θ. The parameter, θ, could index one of a discrete set of alternative models or depict a unknown parameter vector. The decision-maker has a baseline probability $dP_t(\theta)$ for each time instant, t, and makes an adjustment for ambiguity by solving

Problem A.1.

$$\min_{q,\int_\Theta q(\theta)dP_t(\theta)=1} \frac{\partial V}{\partial x'}(x,z)\int_\Theta \mu(x,a\mid\theta)q(\theta)dP_t(\theta) + \chi\int_\Theta q(\theta)\log q(\theta)dP_t(\theta),$$

where χ is a penalty parameter.

This problem is known to have a solution that entails exponential tilting as a function of the drift of the value function for alternative values of θ:

$$q_t^*(\tilde\theta) = \frac{\exp\left(-\frac{1}{\chi}\frac{\partial V}{\partial x'}(X_t)\mu(X_t,A_t\mid\tilde\theta)\right)}{\int_\Theta \exp\left[-\frac{1}{\chi}\frac{\partial V}{\partial x'}(X_t)\mu\left(X_t,A_t\mid\theta\right)\right]dP_t(\theta)}.$$

The minimized objective is

$$-\chi\log\int_\Theta \exp\left[-\frac{1}{\chi}\frac{\partial V}{\partial x'}(x)\mu(x,a\mid\theta)\right]dP_t(\theta). \tag{21}$$

Representation (21) implies an exponential adjustment for model ambiguity concerns.[28] We allow the baseline probability to be time dependent to allow for recursive learning, although we will abstract from this learning in our application.

In constructing Figure 4 we used a variant of this approach solving:

$$\min_{q,\int_\Theta q(\theta)dP_t(\theta)=1} \chi\int_\Theta q(\theta)\log q(\theta)dP_t(\theta)$$

[28] As noted by Hansen and Miao (2018), this exponential adjustment can be viewed as a continuous-time version of a smooth ambiguity adjustment of the type advocated by Klibanoff et al. (2005).

subject to

$$\int_{\Theta} \mu[X_t, a^*(X_t)] q(\theta) dP_t(\theta) = \bar{h}(X_t) \tag{22}$$

where a^* is robustly optimal solution and $\bar{h}$ is deduced from a preference specification with misspecification aversion. We proceed this way to maintain comparability across channels in our analysis of robustness. The minimizing solution takes the form of

$$q_t^*(\theta) \propto \exp\left[-\zeta \mu(X_t, a^*(X_t))\right]$$

and ζ is chosen so that constraint (22) is satisfied.

A.6 Parameter values for the example economy

Parameter	Value
μ_k	0.045
κ	7
σ_k	[0, 0.01]

Table 5: Capital dynamics

Parameter	Value
ζ	0
ψ_0	0.1
ψ_1	0.5
σ_r	[0, 0.0078]

Table 6: Knowledge dynamics

Parameter	Value
α	0.12
$\bar{\beta}$	0.12
$\phi_0(0)$	0.5
ϕ_1	3

Table 7: Productivity

Parameter	Value
δ	.01
ρ	1
ξ	{0.075, 0.15}

Table 8: Preferences

The subjective discount rate is set to $\delta = 0.01$. This value is consistent with the value used by others in the literature, including Barnett et al. (2020, 2022) and Barrage and Nordhaus (2023), and it leads to emissions values in our model that are comparable to estimates of

current and future annual global emissions from Figueres et al. (2018). The baseline choice of the IES is set to $\rho = 1$, which is the standard log utility case. For sensitivity analysis of our model, we examine outcomes for $\rho = 2/3$ and $\rho = 3/2$, which are similar to the values considered for sensitivity analysis by Cai and Lontzek (2019) and others in the literature.

The choices of parameters for the productivity and evolution of productive capital follow from Barnett et al. (2022), who use an undamaged version of the consumption capital model to calibrate the economic growth rate to a value of 2%, consistent with empirical values from the BEA and World Bank databases. The resulting values are set to $\alpha = 0.115, \kappa = 6.667$ and $\mu_k = 0.045$. The capital volatility is set to $\sigma_k = [0, 0.01]$, matching annual percent changes in the time series of GDP from the World Bank database.

Our choices for the emissions component of the production technology (i.e., the abatement cost parameters following the interpretation of Nordhaus and others) are as follows. We set $\phi_1 = 3$, similar to the estimated parameter values from Cai and Lontzek (2019) and Barrage and Nordhaus (2023). While the value of ϕ_0 is highly uncertain, we choose $\phi_0 = 0.5$ as a reasonable benchmark for the fraction of lost output in order to achieve zero emissions. We also consider $\phi_0 = 0.1$, consistent with Barrage and Nordhaus (2023), for a sensitivity analysis comparison. The value for the emissions intensity of output β comes from the implied emissions intensity value for 2020 from Cai and Lontzek (2019).

For the R&D investment parameters, we choose $\psi_1 = 0.5$ for computational tractability and set $\psi_0 = 0.1$ so that our model generates R&D investment values that are in line with major U.S. R&D investment programs as estimated by Stine (2008) and estimates for R&D investment from Bloom et al. (2019). For simplicity, we assume the depreciation of R&D stock is given by $\zeta = 0$. The knowledge stock volatility is set to $\sigma_r = [0, 0.0078]$, matching annual percent changes in the time series of U.S. R&D capital stock from the BLS database.

In our baseline analysis we choose $\xi \in \{0.075, 0.15\}$. As noted previously, the corresponding risk aversion parameters in a recursive utility specification of preferences implied by these values would be $\gamma \approx 7.7$ and $\gamma \approx 14.3$, similar to the values considered by Cai and Lontzek (2019) and others in the literature, and they provide probability distortions that we view as reasonable based on the outcomes reported in Figures 4–7 and Table 2.

The initial value of capital is set so that our initial GDP matches the 2020 World GDP value of $85 trillion estimated by the World Bank National Accounts data. With our choice of $\alpha = 0.115$, we end up with $K_0 = 739.13$. The initial value of knowledge capital is set to

$R_0 = 11.2/1120$, which converts and scales the value for current US R&D capital stock in the BLS database to a global value such that the expected arrival time of a breakthrough green technological change without additional R&D investment is the year 2100. The initial value of atmospheric temperature anomaly is set to $Y_0 = 1.1$ degrees Celsius to match recent estimates from the IPCC AR6.

B Marginal value function derivations

This section of the Appendix fills in some details of value function derivative representations.

B.1 Infinitesimal generators of interest

Our approach is to feature explicitly the Brownian motion contributions prior to any jumps taking place. We capture the impact of jumps through the continuation values conditioned on each of the jump types, $\ell = 1, ..., L$. We represent jump prospects by an implied state-dependent discount factor process.

We find it convenient to work with infinitesimal generators to deduce the formulas of interest. Let $\mathbb{A}$ be the familiar (extended) generator for the process X given by

$$\mathbb{A}\psi(x) \stackrel{\text{def}}{=} \mu(x) \cdot \frac{\partial \psi}{\partial x}(x) + \frac{1}{2}\text{trace}\left[\sigma(x)' \frac{\partial^2 \psi}{\partial x \partial x'}(x)\sigma(x)\right].$$

Using this operator notation, we rewrite equation (6) compactly as:

$$\delta U + \sum_{\ell=1}^{L} \mathcal{J}^\ell V^\ell - \delta V - \sum_{\ell=1}^{L} \mathcal{J}^\ell V + \mathbb{A}V = 0 \tag{23}$$

Given formulas (9) and (10), we build a generator $\mathbb{B}$ for the composite state vector (X, M) process such that

$$\mathbb{B}\psi(x^b) \stackrel{\text{def}}{=} \mu^b(x^b) \cdot \frac{\partial \psi}{\partial x^b}(x^b) + \frac{1}{2}\text{trace}\left[\sigma^b(x^b)' \frac{\partial^2 \psi}{\partial x^b \partial x^{b\prime}}(x^b)\sigma^b(x^b)\right]$$

where $x^b = (x, m)$ denotes the composite state vector.

We are interested in representing $\mathbb{B}$ for a particular class of functions of (x, m) of the form

$$\Phi(x) \cdot m$$

where

$$\Phi = \frac{\partial \phi}{\partial x}$$

for a (smooth) scalar function ϕ of x. We construct $\mathbb{A}_{x_i}$ as

$$\mathbb{A}_{x_i}\Phi(x) \stackrel{\text{def}}{=} \frac{\partial \mu}{\partial x_i}(x) \cdot \frac{\partial \phi}{\partial x}(x) + \frac{1}{2}\text{trace}\left[\frac{\partial \sigma}{\partial x_i}(x)' \frac{\partial^2 \phi}{\partial x \partial x'}(x)\sigma(x) + \sigma(x)' \frac{\partial^2 \phi}{\partial x \partial x'}(x)\frac{\partial \sigma}{\partial x_i}(x)\right].$$

Then by essentially just applying the product rule for derivatives we get

$$\mathbb{B}\left[\Phi(x) \cdot m\right] = \mathbb{A}\Phi(x) \cdot m + \left[\mathbb{A}_x \phi\right] \cdot m.$$

Now differentiate the Feynman-Kac equation (23) with respect to each coordinate and form the dot product with m to obtain

$$\delta m \cdot \frac{\partial U}{\partial x} + m \cdot \left[\sum_{\ell=1}^{L} \mathcal{J}^\ell \frac{\partial V^\ell}{\partial x} + \left(V^\ell - V\right) \frac{\partial \mathcal{J}^\ell}{\partial x}\right] - \left[\delta + \sum_{\ell=1}^{L} \mathcal{J}^\ell\right] m \cdot \frac{\partial V}{\partial x} + \mathbb{B}\left[\frac{\partial V}{\partial x} \cdot m\right] = 0.$$

Equivalently,

$$\begin{aligned} V_{x_i}(x) =& \delta \int_0^\infty \mathbb{E}\left[\exp\left(-\int_0^t \left[\delta + \sum_{\ell=1}^{L} \mathcal{J}^\ell(X_u)\right] du\right)\left(\delta M_t \cdot \frac{\partial U}{\partial x}(X_t)\right.\right. \\ &\left.\left. + M_t \cdot \sum_{\ell=1}^{L}\left[\mathcal{J}^\ell(X_t)\frac{\partial V^\ell}{\partial x}(X_t) + \left[V^\ell(X_t) - V(X_t)\right]\frac{\partial \mathcal{J}^\ell}{\partial x}(X_t)\right]\right) \mid X_0 = x, M_0 = \mathbf{e}_i\right] dt \end{aligned}$$

where $\mathbf{e}_i$ is the i^{th} coordinate vector in $\mathbb{R}^n$.

B.2 Extension to accommodate robustness

We next consider implications of aversion to misspecification by entertaining a general class of class of drift distortions. We initially explore the consequences of exogenous-specified drift distortion, and then we demonstrate how to make this distortion reflect misspecification

aversion.

B.2.1 Exogenous drift distortion

We introduce an exogenously specified drift distortion process H into the diffusion dynamics:

$$\begin{aligned} dX_t &= \mu(X_t)dt + \sigma(X_t)H\left(\overline{X}_t\right)dt + \sigma(X_t)dW_t \\ d\overline{X}_t &= \bar{\mu}\left(\overline{X}_t\right)dt + \bar{\sigma}\left(\overline{X}_t\right)dW_t. \end{aligned}$$

By imitating our previous analysis, we associate with this joint system $(X, \overline{X})$ a composite variational process $(M, \overline{M})$. Given interest in endogenous state variable sensitivity, it is the M component that interests us and not the $\overline{M}_t$ process. Notice that if we set $\overline{M}_0 = 0$, then $\overline{M}_t = 0$ for $t > 0$.

The evolution for the variational process component M is now:

$$dM_t^i = (M_t)' \left[\frac{\partial \mu_i}{\partial x}(X_t) + \frac{\partial \sigma_i}{\partial x}(X_t)H\left(\overline{X}_t\right)\right]dt + (M_t)'\frac{\partial \sigma_i}{\partial x}(X_t)dW_t.$$

Importantly, there is no contribution from differentiating H with respect to x since H only depends on the $\overline{X}_t$ process.

Remark B.1. *While we focus on Markov forms of misspecification, this can be relaxed. The misspecification that will turn out to be most concerning to the decision maker will have a Markov representation, which is why we make the Markov restriction here.*

B.2.2 Value function derivatives under robustness

We next explore two value function constructions. We include one with a drift distortion governed by exogenous dynamics for purposes of interpretation. The second one we consider streamlines the computations. As we will show there is a convenient link between these two value functions.

For the first construction, we let the flow term be:

$$\delta U(x) + \frac{\xi}{2}|H\left(\bar{x}\right)|^2.$$

This implies a value function $\overline{V}(x, \bar{x})$.

The second value function used for computing a robustness adjustment to valuation coincides with what is used in robust control formulations. The value function is given as a solution to the HJB equation:

$$0 = \min_h \delta U(x) - \delta V(x) + \frac{\xi}{2}|h|^2 + [\mu(x) + \sigma(x)h]\, V_x(x) + \frac{1}{2}\text{trace}\left[\sigma(x)' V_{xx}(x)\sigma(x)\right]. \quad (24)$$

The first-order conditions for h in equation (24) imply that

$$\sigma(x)' V_x(x) + \xi h = 0$$

The HJB solution, V, also satisfies the FK equation when we substitute the minimizing h into the HJB equation.

$$0 = \delta U(x) - \delta V(x) + \frac{\xi}{2}|h^*(x)|^2 + [\mu(x) + \sigma(x)h^*(x)] \cdot V_x(x) + \frac{1}{2}\text{trace}\left[\sigma(x)' V_{xx}(x)\sigma(x)\right] \quad (25)$$

where

$$h^*(x) = -\frac{1}{\xi}\sigma'(x)V_x(x) \quad (26)$$

Consider the exogenously specified drift distortion as in the previous subsection where $H = h^*$ and $\bar{X}$ stochastic dynamics satisfy the consistency requirement:

$$\begin{aligned} \bar{\mu}(x) &= \mu(x) + H(x) \\ \bar{\sigma}(x) &= \sigma(x) \end{aligned}$$

and $\bar{X}_0 = X_0$. Thus along a stochastic path, $\overline{X}_t = X_t$.

We next show that

$$\begin{aligned} V(x) &= \overline{V}(x, x) \\ V_x(x) &= \overline{V}_x(x, x) \end{aligned} \quad (27)$$

when

$$H(\bar{x}) = h^*(\bar{x}) \quad (28)$$

Note that it follows from the second equation in (27) that

$$V_{xx}(x) = \overline{V}_{xx}(x,x) + \overline{V}_{x\bar{x}}(x,x)$$

Differentiate equation (25) with respect to x:

$$\begin{aligned} 0 = & -\delta V_x + \delta U_x + V_{xx}\left(\mu + \sigma h^*\right) + (\mu_x)' V_x + \text{mat}\left\{\left(\frac{\partial \sigma_i}{\partial x}\right) h^*\right\}' V_x \\ & + \frac{\partial}{\partial x}\left[\frac{1}{2}\text{trace}\left(\sigma' V_{xx}\sigma\right)\right] \end{aligned}$$

where mat denotes a matrix formed by stacking the column arguments. This expression uses the first-order conditions for h to cancel out terms (Envelope Theorem).

We repeat the same differentiation for $\overline{V}$ with respect to the first-argument and then substitute $x = \bar{x}$ to obtain (27) provided that we set $H(x) = h^*(x)$.

Remark B.2. *Observe the specification of the drift distortion in terms of the exogenous dynamics provides an substantive interpretation of our application of the Envelope Theorem. Recall that we used the Envelope Theorem to omit certain derivatives associated with minimization in our construction of* V*. When we use* (28) *with the* $\bar{x}$ *argument, such derivatives do not play a role when in the solution for* $\overline{V}$*. Using the exogenous dynamics to characterize the drift distortion also simplifies our interpretation of the uncertainty-adjusted probability measure that we feature in our analysis.*

Remark B.3. *We could drop* $\frac{\xi}{2}|H\left(\overline{X}_t\right)|^2$ *from the flow term used in constructing* $\overline{V}$ *and still obtain the second equality in* (27) *involving first-derivatives of value functions. We will need to include an analogous term, however, once we entertain jumps.*

Remark B.4. *While we demonstrate that we may treat the drift distortion as exogenous to the original state dynamics, for some applications we may wish to view it as a change in the endogenous dynamics as is reflected* (26)*.*

B.2.3 Jump contributions

As we noted previously, we incorporate jumps by including contributions that are expressed in terms of continuation value functions conditioned on each jump. This approach introduced

supplementary flow terms or social payoffs, in addition to $\frac{\partial U}{\partial x}(X_t)$, into the analysis. Robustness concerns applied to jumps add additional adjustments into each of the intensities, the $\mathcal{J}^\ell$'s, captured by the g^ℓ's. As with drift distortions we may capture these as functions of the exogenous state $\overline{X}$. With minimization subject to a relative entropy penalty, we may again apply the Envelope Theorem to connect the counterparts to the value functions V and $\overline{V}$. For instance, this is why we exclude partial derivatives of $g^{\ell *}$ with respect to the state vector x in the contribution:

$$\sum_{\ell=1}^{L} \left[\mathcal{J}_x^\ell(X_t) g^{\ell *}(X_t) \left[V^\ell(X_t) - V(X_t)\right] + \mathcal{J}^\ell(X_t) g^{\ell *}(X_t) V_x^\ell(X_t)\right].$$

While the relative entropy penalty may be dropped for the drift contributions, the same is not true for the jump contributions:

$$\xi \sum_{\ell=1}^{L} \mathcal{J}_x^\ell(X_t) \left[1 - g^{\ell *}(X_t) + g^{\ell *}(X_t) \log g^{\ell *}(X_t)\right]$$

This is because the endogenous state variables are arguments in the jump intensity functions.

B.3 Valuation decompositions with alternative configurations of uncertainty aversion

Recall that Table 4 in Section 8.1 featured only uncertainty about the R&D technology and set $\xi = .15$. We now explore the implications three alternatives.

Table 9, reports the corresponding results when all four channels are activated while leaving $\xi = .15$. While the numerical magnitudes changed, the overall characterizations still apply.

	i	ii	iii(dc)	iii(td)	iv	sum
pre neutrality						
a) post neutrality	0.0019	0.0129	0.0136	0.0017	0.0000	0.0300
b) post aversion	0.0026	0.0151	0.0158	0.0028	0.0000	0.0363
pre aversion						
c) post neutrality	0.0021	0.0099	0.0170	0.0013	0.0029	0.0331
d) post aversion	0.0031	0.0101	0.0219	0.0021	0.0046	0.0417

Table 9: Components to the partial derivative of the value function with respect to the R&D state variable. The column iii(dc) includes only the contributions from the damage curve realization jumps to iii, and iii(td) includes the remaining contribution from the technology discovery jump to iii. All four uncertainty channels are activated, and uncertainty aversion is set to $\xi = 0.15$.

We next activate only the R&D technology discovery channel and consider the implications of increasing uncertainty aversion by setting $\xi = .075$. The results for this case are given in Table 10. The qualitative patterns remain similar to those in Table 4, but the quantitative magnitudes have now changed.

	i	ii	iii(dc)	iii(td)	iv	sum
pre neutrality						
a) post neutrality	0.0019	0.0129	0.0136	0.0017	0.0000	0.0300
b) post aversion	0.0035	0.0208	0.0171	0.0039	0.0000	0.0453
pre aversion						
c) post neutrality	0.0019	0.0067	0.0184	0.0008	0.0042	0.0321
d) post aversion	0.0034	0.0063	0.0294	0.0012	0.0102	0.0505

Table 10: Components to the partial derivative of the value function with respect to the R&D state variable. The column iii(dc) includes only the contributions from the damage curve realization jumps to iii, and iii(td) includes the remaining contribution from the technology discovery jump to iii. Only the R&D uncertainty channel is activated, and uncertainty aversion is set to $\xi = 0.075$.

Finally, we again only activate uncertainty concerns about the R&D technology discovery

channel and consider the implications of increasing uncertainty aversion to a substantially more extreme value by setting $\xi = .005$. The results for this case are given in Table 11. This changes both the quantitative and qualitative results in comparison to 4. The marginal value of the R&D investment is substantially lower in comparison to a neutrality benchmark. We will have more to say about this case in Section D.1.

	i	ii	iii(dc)	iii(td)	iv	sum
pre neutrality						
post neutrality	0.0019	0.0129	0.0136	0.0017	0.0000	0.0300
post aversion	0.0096	0.0719	0.0012	0.0224	0.0000	0.1051
pre aversion						
post neutrality	0.0013	−0.0003	0.0238	0.0000	0.0015	0.0262
post aversion	−0.0013	−0.0002	0.0109	0.0000	0.0020	0.0114

Table 11: Components to the partial derivative of the value function with respect to the R&D state variable. The column iii(dc) includes only the contributions from the damage curve realization jumps to iii, and iii(td) includes the remaining contribution from the technology discovery jump to iii. Only the R&D uncertainty channel is activated, and uncertainty aversion is set to $\xi = 0.005$.

C State and control variables

We have one technology jump and $L-1$ damage jumps. Thus there are L states to jump to initially. Let the first jump state be an R&D discovery. When a jump of type L happens, the state x jumps to $\bar{x}^{\ell}(x)$. For a technology jump, $\bar{x}^{L}(x)$ simply drops the technology state and leaves the remainder the same. For all of the damage jumps, $\bar{x}^{\ell}(x)$ replaces y by $\overline{y}$ and leaves the remaining components of x the same. In our parameterization of the intensities, we use one of the following expressions depending on the type of jump being considered:

$$\mathcal{J}^{\ell}(x) = \left(\frac{1}{1-L}\right)\mathcal{J}^{n}(y),\ \ell = 1, 2, ..., L-1,$$

and

$$\mathcal{J}^{L}(x) = r.$$

We compute our continuation values using a version of backward induction.

i) Compute $V^{\ell,L}(x)$ for $\ell = 1, ..., L-1$ conditioned on both a technology jump and a damage jump occurring. This value function does not depend on the R&D state variable.

ii) Compute the values functions $V^{\ell}(x)$ assuming that only a damage jump has been realized for $\ell = 1, ..., L-1$. These values functions depend on the entire state vector x and have one possible jump state which is the technology discovery with intensity $\mathcal{J}^L$. The continuation value for the jump is $V^{\ell,L}(x)$ viewed as a function of x for $\ell = 1, ..., L-1$.

iii) Compute the value function $V^L(x)$ assuming that only a technology jump has been realized. This value function incorporates the possibility of jumping to one of $L-1$ possible damage states, however, because the temperature anomaly remains constant at the point where any incremental curvature has no impact on the damages this damage curve realization is inconsequential. Therefore, we can ignore the damage curve intensities and the associated continuation values for this computation.

iv) Compute $V(x)$ prior to any jumps occurring. This value function has two possible types of jumps, either a technology jump or a damage curvature jump. The continuation value for the technology jump is $V^L(x)$, and the potential continuation values for the damage curvature jump are the set of $V^{\ell}(x)$ for $\ell = 1, ..., L-1$.

With respect to the jump state Z and its evolution process mentioned in Section 4.1, we represent Z as the ordered pair $Z = (z_n, z_r)$. The first component, z_n, is in the set $\{0, 1, 2, ..., L-1\}$, where the L realizations depict either no damage curve jump having occurred for the value of zero or one of the $L-1$ possible damage curves for $\ell \in \{1, 2, ..., L-1\}$. The second component, z_r, is the technology state and is equal to zero or one, where zero is the technology state prior to a new discovery and one is the state after the discovery. Thus there are $2L$ possible pairs for the jump state Z.

The states $\bar{x}^{\ell}(x)$ and Z are subsumed within the value function notation used above. Therefore, the value functions corresponding to the different jump states outlined above can

be written as explicit functions of the states as follows:

$$\begin{aligned} V^{\ell,L}(x) &= V(\bar{x}^{\ell},(\ell,L)), \\ V^{\ell}(x) &= V(\bar{x}^{\ell},(\ell,0)), \\ V^{L}(x) &= V(\bar{x}^{\ell},(0,L)), \\ V(x) &= V(x,(0,0)). \end{aligned}$$

Note that $\mathcal{J}^{\ell}$ is a composite intensity of a first jump, either a technology jump or a jump to one of damage curvature states. Since the first jump could be one of two types, the jump probabilistic transitions for either jump type occurring is given by

$$\left(\frac{1}{L-1}\right)\mathcal{J}^{n}(y)+r$$

The respective jump probabilistic transitions for either a damage curvature jump or a technology jump are given by the intensity fractions

$$\frac{\mathcal{J}^{n}(y)/(L-1)}{r+\mathcal{J}^{n}(y)/(L-1)} \quad \frac{r}{r+\mathcal{J}^{n}(y)/(L-1)}.$$

C.1 HJB Equation for $\rho \neq 1$

Below we write out explicitly the HJB equation and quasi-analytical simplification for the pre-technological change, pre-damage function jump state when $\rho \neq 1$. The special case for $\rho = 1$ is entirely similar. Starting from Equation (20),

$$0 = \frac{\delta}{1-\rho}\left[\left(\frac{C_t}{\exp(V_t)}\right)^{1-\rho}-1\right]+\frac{dV_t}{dt} \tag{29}$$

and applying equation (13) and the expression for $\frac{dV_t}{dt}$ gives rise to the HJB equation:

$$
\begin{aligned}
0 \;=\; & \max_{I^k, I^r, \mathcal{E}} \min_{h, g^\ell} \frac{\delta}{1-\rho} \left(\left(\frac{\alpha k - I^k - I^r - \alpha k \phi_0(z) \left(1 - \frac{\mathcal{E}}{\beta \alpha k}\right)^{\phi_1}}{\exp(V) n} \right)^{1-\rho} - 1 \right) \\
& + \frac{\partial V}{\partial \hat{k}} \left(-\mu_k + \frac{I^k}{k} - \frac{\kappa}{2} \left(\frac{I^k}{k} \right)^2 - \frac{|\sigma_k|^2}{2} + \sigma_k h \right) + \frac{\partial^2 V}{\partial \hat{k} \, \partial \hat{k}'} \frac{|\sigma_k|^2}{2} \\
& + \frac{\partial V}{\partial y} \mathcal{E} \left(\bar{\theta} + \varsigma h \right) + \frac{\partial^2 V}{\partial y \, \partial y'} \frac{|\varsigma|^2}{2} \mathcal{E}^2 \\
& + \frac{\partial V}{\partial \hat{n}} \left((\lambda_1 + \lambda_2 y) \mathcal{E} \left(\bar{\theta} + \varsigma h \right) + \lambda_2 \frac{|\varsigma|^2}{2} \mathcal{E}^2 \right) + \frac{\partial^2 V}{\partial \hat{n} \, \partial \hat{n}'} \frac{(\lambda_1 + \lambda_2 y)^2 |\varsigma|^2}{2} \mathcal{E}^2 \\
& + \frac{\partial V}{\partial \hat{r}} \left(-\zeta + \psi_0 (I^r)^{\psi_1} \exp(-\psi_1 \hat{r}) - \frac{|\sigma_r|^2}{2} + \sigma_r h \right) + \frac{\partial^2 V}{\partial \hat{r} \, \partial \hat{r}'} \frac{|\sigma_r|^2}{2} \\
& + \sum_{\ell=1}^{L} \mathcal{J}^\ell g^\ell \left[V^\ell - V \right] + \xi \sum_{\ell=1}^{L} \mathcal{J}^\ell \left[1 - g^\ell + g^\ell \log g^\ell \right] + \frac{\xi}{2} h' h,
\end{aligned}
$$

where we have allowed for the various types of uncertainty outlined previously.

The solution has a quasi-analytical simplification of the form

$$V(X_t) = \hat{V}(X_t^1) - \hat{N}.$$

After plugging this simplification into our HJB equation and removing common terms,

we are left with the following simplified HJB to solve:

$$
\begin{aligned}
0 \;=\; & \max_{I^k, I^r, \mathcal{E}} \min_{h, g^\ell} \frac{\delta}{1-\rho} \left(\left(\frac{\alpha k - I^k - I^r - \alpha k \phi_0(z) \left(1 - \frac{\mathcal{E}}{\beta \alpha k}\right)^{\phi_1}}{\exp(\hat{V})} \right)^{1-\rho} - 1 \right) \\
& + \frac{\partial \hat{V}}{\partial \hat{k}} \left(-\mu_k + \frac{I^k}{k} - \frac{\kappa}{2} \left(\frac{I^k}{k} \right)^2 - \frac{|\sigma_k|^2}{2} + \sigma_k h \right) + \frac{\partial^2 \hat{V}}{\partial \hat{k} \, \partial \hat{k}'} \frac{|\sigma_k|^2}{2} \\
& + \frac{\partial \hat{V}}{\partial y} \mathcal{E} \left(\bar{\theta} + \varsigma h \right) + \frac{\partial^2 \hat{V}}{\partial y \, \partial y'} \frac{|\varsigma|^2}{2} \mathcal{E}^2 - \left((\lambda_1 + \lambda_2 y) \mathcal{E} \left(\bar{\theta} + \varsigma h \right) + \lambda_2 \frac{|\varsigma|^2}{2} \mathcal{E}^2 \right) \\
& + \frac{\partial \hat{V}}{\partial \hat{r}} \left(-\zeta + \psi_0 (I^r)^{\psi_1} \exp(-\psi_1 \hat{r}) - \frac{|\sigma_r|^2}{2} + \sigma_r h \right) + \frac{\partial^2 \hat{V}}{\partial \hat{r} \, \partial \hat{r}'} \frac{|\sigma_r|^2}{2} \\
& + \sum_{\ell=1}^{L} \mathcal{J}^\ell g^\ell \left[\hat{V}^\ell - \hat{V} \right] + \xi \sum_{\ell=1}^{L} \mathcal{J}^\ell \left[1 - g^\ell + g^\ell \log g^\ell \right] + \frac{\xi}{2} h' h.
\end{aligned}
$$

This HJB equation characterizes only the pre-technological change, pre-damage function jump state, but the simplifications used carry through for each of the corresponding post-jump states needed to solve the full problem. The HJB equations characterizing those jump states are similar, with adjustments made for the realization of each of the jump processes.

D Parameter sensitivity

In this section of the appendix we explore sensitivity to some our parametric inputs.

D.1 Non-monotonic response to uncertainty aversion

From our comparison of outcomes across different levels of uncertainty aversion in Section 7.3.1 we see that R&D investment increases as potential misspecification aversion increases. Expanding our sensitivity analysis to include outcomes for $\xi = 0.005$, shown in Figure 11, we see there is a non-monotonic response of R&D investment to sufficiently large increases in the aversion to misspecification uncertainty. The R&D investment-output, shown in Panel A, drops down to near zero for $\xi = 0.005$, as the implied worst-case probabilities of the social planner are such that the robustly optimal policy choice is to respond as if a technological

innovation discovery is very unlikely to be realized for the planner's relevant decision-making horizon.

The robustly optimal policy response of emissions, shown in Panel B, now imposes a significantly stronger reduction as compared to the baseline values of ξ. The initial value of emissions is nearly cut in half compared to the values observed for neutral, less, and more aversion cases, and the pathway is gradually decreasing over the 30 year horizon. This finding is due in large part to the imposition of this more extreme aversion to all four channels. Figure 12 only activates the R&D technology discovery channel and finds a much more muted emissions response.

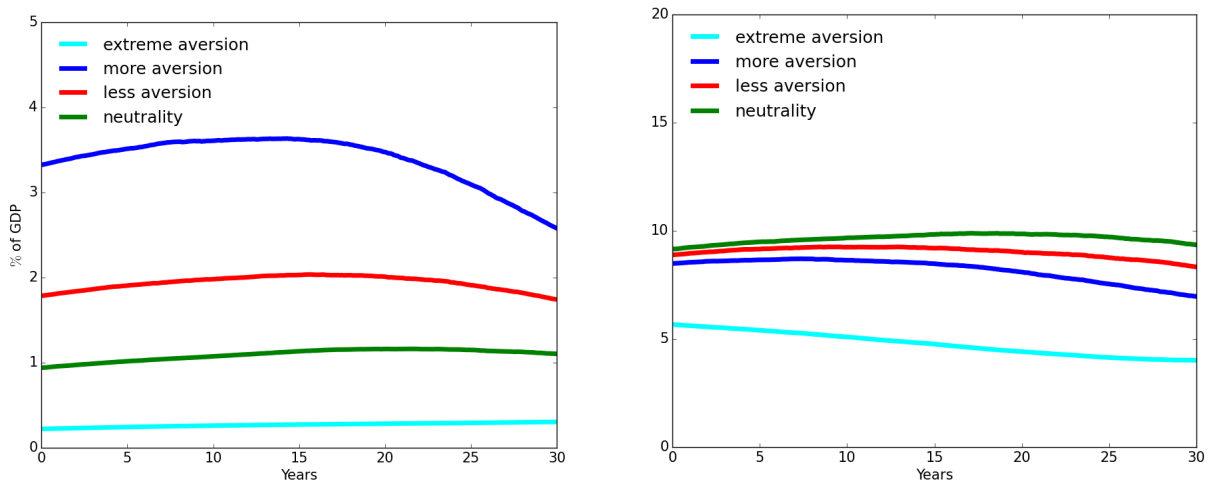

(A) R&D investment

(B) Emissions

Figure 11: Simulated expected pathways of R&D investment as a fraction of output and emissions in gigatons of carbon (GtC). Panel A compares outcomes of R&D investment for different values of the misspecification aversion parameter ξ. Panel B compares outcomes of emissions for different values of the misspecification aversion parameter ξ. The trajectories are simulated under the baseline transition dynamics averaging over Brownian and jump shocks. All four uncertainty channels are activated.

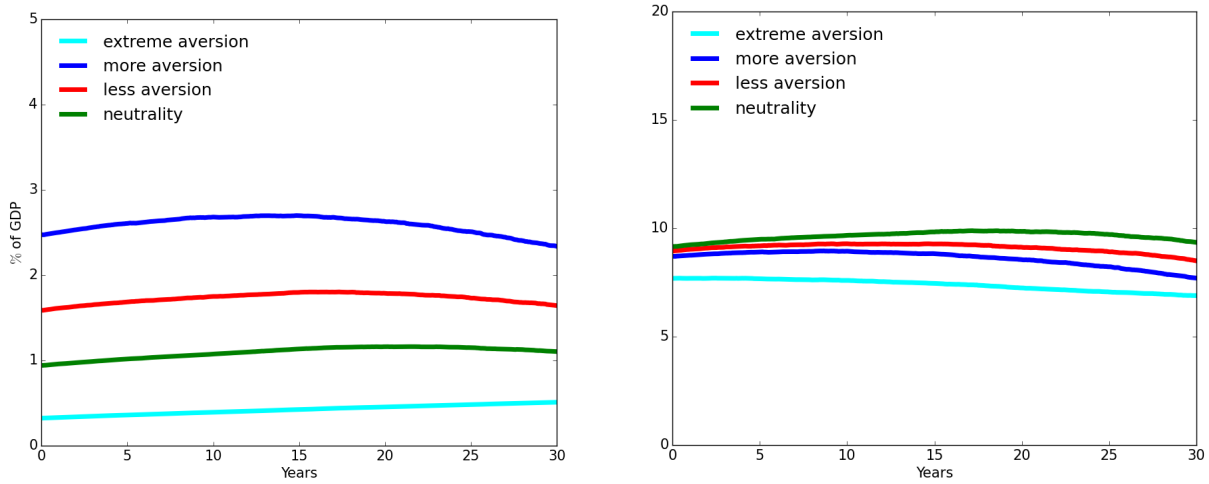

(A) R&D investment

(B) Emissions

Figure 12: Simulated expected pathways of R&D investment as a fraction of output and emissions in gigatons of carbon (GtC). Panel A compares outcomes of R&D investment for different values of the misspecification aversion parameter ξ. Panel B compares outcomes of emissions for different values of the misspecification aversion parameter ξ. The trajectories are simulated under the baseline transition dynamics averaging over Brownian and jump shocks. Only the R&D uncertainty channel is activated.

D.2 Increasing the subjective rate of discount

In our baseline analysis, we have kept fixed the subjective rate of discount used by the social planner by setting $\delta = .01$. We now show how changes in this subjective discount rate alters the social value of the R&D stock and the social cost of global warming. In Table 12 we report computations for both the social value of R&D and the social cost of global warming, showing drops in the both social valuations. Since the reported numbers are in a logarithmic scale, we see drops in the valuations by about 30% by increasing δ from .01 to .015, and by an additional 30% to nearly 40% when increasing δ to .02.

D.3 Intertemporal elasticity of substitution (IES)

We next consider two other specifications of the IES that differ from unity: $\rho = 2/3$ and $\rho = 3/2$. We show these results in Table 13. As noted previously in relation to growth models, the investment in both types of capital relative to output are higher when the elasticity is

Subjective discount rate	$\log SVRD$	$\log SCGW$
$\delta = .010$	6.79	11.61
$\delta = .015$	6.46	11.33
$\delta = .020$	6.07	11.01

Table 12: Social values at the initial time period for less aversion to misspecification uncertainty.

greater (ρ is smaller). Table 14 shows the (log) social value of the R&D stock and the (log) social cost of global warming for $\rho = 2/3$, $\rho = 1$, and $\rho = 3/2$. Consistent with expectations noted earlier, the valuations of the corresponding capital stocks move in the opposite way.

	R&D-output ratio			Investment-output ratio		
Uncertainty aversion	$\rho = 2/3$	$\rho = 1$	$\rho = 3/2$	$\rho = 2/3$	$\rho = 1$	$\rho = 3/2$
more aversion	7.6%	3.5%	1.5%	88.7%	74.3%	66.5%
less aversion	4.6%	1.8%	0.8%	92.3%	76.0%	67.3%
neutrality	2.8%	1.0%	0.4%	94.6%	77.0%	67.6%

Table 13: Initial investment to output ratios for different specifications of the IES.

IES	$\log SVRD$	$\log SCGW$
$\rho = 2/3$	4.89	9.71
$\rho = 1$	6.79	11.61
$\rho = 3/2$	6.86	11.75

Table 14: Social values at the initial time period for less aversion to misspecification uncertainty.

D.4 Abatement technology sensitivity

One of important parameters choices in our framework is the choice of abatement technology parameter ϕ_0. In the table and remark that follow, we elaborate on how changing the value of ϕ_0 impacts our model results across different cases of model uncertainty aversion.

As we noted in Remark 4.1, economic models of climate change often make reference to an "abatement technology." We instead start with a production function that includes a

	R&D-output ratio		emissions	
Uncertainty aversion	$\phi_0 = .5$	$\phi_0 = .1$	$\phi_0 = .5$	$\phi_0 = .1$
More Aversion	3.52%	1.20%	8.44	6.75
Less Aversion	1.85%	0.94%	8.86	7.43
Neutrality	0.97%	0.44%	9.14	8.18

Table 15: Initial robust actions for two alternative initial specifications of ϕ_o.

specific role for fossil fuels as an input. There is a loss in output when this input is reduced, which could be labeled as abatement. In the extreme case in which $\mathcal{E}_t = 0$, the fraction of output remaining is $1 - \phi_0(Z_t)$. Previous work by Nordhaus and others assumes $\phi_0 \leqslant .1$ net of technological progress. In our example, ϕ_0 is initially .5, which implies a substantially larger measure of the production cost of decarbonization than other literature, albeit one that we find to be more substantively relevant. The results are indeed sensitive to this aspect of our example specification.

Since the output loss induced by a reduction in emissions would be substantially lower when ϕ_0 is initialized at .1 instead of .5, this change leads to i) substantially less R&D as a fraction of output and ii) a more modest but notable proportional reduction in emissions. We illustrate this in Table 15.

References

Abel, Andrew B. 1983. Optimal investment under uncertainty. *The American Economic Review* 73 (1):228–233.

Acemoglu, Daron, Ufuk Akcigit, Douglas Hanley, and William Kerr. 2016. Transition to clean technology. *Journal of Political Economy* 124 (1):52–104.

Anderson, Evan W, Lars Peter Hansen, and Thomas J Sargent. 2003. A quartet of semigroups for model specification, robustness, prices of risk, and model detection. *Journal of the European Economic Association* 1 (1):68–123.

Bansal, Ravi and Amir Yaron. 2004. Risks for the Long Run: A Potential Resolution of Asset Pricing Puzzles. *Journal of Finance* 59 (4):1481–1509.

Bansal, Ravi, Dana Kiku, and Marcelo Ochoa. 2019. Climate change risk. *Federal Reserve Bank of San Francisco Working Paper* .

Barnett, Michael. 2023. Climate change and uncertainty: An asset pricing perspective. *Management Science* .

Barnett, Michael, William A. Brock, and Lars Peter Hansen. 2020. Pricing Uncertainty Induced by Climate Change. *Review of Financial Studies* 33 (3):1024–1066.

Barnett, Michael, William Brock, and Lars Peter Hansen. 2022. Climate change uncertainty spillover in the macroeconomy. *NBER Macroeconomics Annual* 36 (1):253–320.

Barrage, Lint and William D Nordhaus. 2023. Policies, Projections, and the Social Cost of Carbon: Results from the DICE-2023 Model. Tech. Rep. w31112, NBER.

Berger, Loic and Massimo Marinacci. 2020. Model Uncertainty in Climate Change Economics: A Review and Proposed Framework for Future Research. *Environmental and Resource Economics* 1–27.

Bloom, Nicholas and John Van Reenen. 2002. Patents, real options and firm performance. *The Economic Journal* 112 (478):C97–C116.

Bloom, Nicholas, John Van Reenen, and Heidi Williams. 2019. A toolkit of policies to promote innovation. *Journal of Economic Perspectives* 33 (3):163–84.

Bloom, Nick, Stephen Bond, and John Van Reenen. 2007. Uncertainty and investment dynamics. *The review of economic studies* 74 (2):391–415.

Bolton, Patrick, Neng Wang, and Jinqiang Yang. 2019. Investment under uncertainty with financial constraints. *Journal of Economic Theory* 184:104912.

Borovička, Jaroslav, Lars Peter Hansen, and Jose A. Scheinkman. 2014. Shock Elasticities and Impulse Responses. *Mathematics and Financial Economics* 8 (4).

Brock, W. and A. Xepapadeas. 2017. Climate change policy under polar amplification. *European Economic Review* 99:263–282.

Brook, Barry W., Erle C. Ellis, Michael P. Perring, Anson W. Mackay, and Linus Blomqvist. 2013. Does the terrestrial biosphere have planetary tipping points? *Trends in Ecology and Evolution* 28:396–401.

Cai, Yongyang and Thomas S Lontzek. 2019. The social cost of carbon with economic and climate risks. *Journal of Political Economy* 127 (6):2684–2734.

Cai, Yongyang, Kenneth L. Judd, and Thomas S. Lontzek. 2017. The Social Cost of Carbon with Climate Risk. Tech. rep., Hoover Institution, Stanford, CA.

Cappelli, Veronica, Simone Cerreia-Vioglio, Fabio MacCheroni, Massimo Marinacci, and Stefania Minardi. 2021. Sources of Uncertainty and Subjective Prices. *Journal of the European Economic Association* 19:872–912.

Cerreia-Vioglio, Simone, Lars Peter Hansen, Fabio Maccheroni, and Massimo Marinacci. 2021. Making Decisions under Model Misspecification.

Chang, Kenneth. 2022. Scientists Achieve Nuclear Fusion Breakthrough With Blast of 192 Lasers. *New York Times, December 13* .

Dixit, Avinash K and Robert S Pindyck. 1994. *Investment under uncertainty*. Princeton university press.

Duffie, D and L G Epstein. 1992. Stochastic Differential Utility. *Econometrica* 60:353–394.

Epstein, Larry G. and Stanley E. Zin. 1989. Substitution, Risk Aversion and the Temporal Behavior of Consumption and Asset Returns: A Theoretical Framework. *Econometrica* 57 (4):937–969.

Figueres, Christiana, Corinne Le Quéré, Anand Mahindra, Oliver Bäte, Gail Whiteman, Glen Peters, and Dabo Guan. 2018. Emissions Are Still Rising: Ramp Up the Cuts. *Nature* 564:27–30.

Fournie, E, J M Lasry, J Lebuchoux, P L Lions, and N Touzi. 1999. Applications of Malliavin Calculus to Monte Carlo Methods in Finance. *Finance and Stochastics* 3:391–413.

Geoffroy, O, D Saint-Martin, D J L Olivié, A Voldoire, G Bellon, and S Tytéca. 2013. Transient Climate Response in a Two-Layer Energy-Balance Model. Part I: Analytical Solution and Parameter Calibration Using CMIP5 AOGCM Experiments. *Journal of Climate* 26 (6):1841–1857.

Hambel, Christoph, Holger Kraft, and Eduardo Schwartz. 2021. Optimal carbon abatement in a stochastic equilibrium model with climate change. *European Economic Review* 132:103642.

Hansen, Lars Peter and Jianjun Miao. 2018. Aversion to Ambiguity and Model Misspecification in Dynamic Stochastic Environments. *Proceedings of the National Academy of Sciences* 115 (37):9163–9168.

Hansen, Lars Peter and Thomas J. Sargent. 1995. Discounted Linear Exponential Gaussian Control. *IEEE Transactions on Automatic Control* 40:968–971.

———. 2001. Robust Control and Model Uncertainty. *The American Economic Review* 91 (2):60–66.

Hennlock, Magnus. 2009. Robust Control in Global Warming Management: An Analytical Dynamic Integrated Assessment. Tech. Rep. 9-19, RFF Discussion Paper.

Jaakkola, Niko and Frederick van der Ploeg. 2019. Non-cooperative and cooperative climate policies with anticipated breakthrough technology. *Journal of Environmental Economics and Management* 97:42–66.

Jacobson, David H. 1973. Optimal Stochastic Linear Systems with Exponential Performance Criteria and Their Relation to Deterministic Differential Games. *IEEE Transactions for Automatic Control* AC-18:1124–1131.

Joos, F., R. Roth, J. S. Fuglestvedt, G. P. Peters, I. G. Enting, W. Von Bloh, V. Brovkin, E. J. Burke, M. Eby, N. R. Edwards, T. Friedrich, T. L. Frölicher, P. R. Halloran, P. B. Holden, C. Jones, T. Kleinen, F. T. Mackenzie, K. Matsumoto, M. Meinshausen, G. K. Plattner, A. Reisinger, J. Segschneider, G. Shaffer, M. Steinacher, K. Strassmann, K. Tanaka, A. Timmermann, and A. J. Weaver. 2013. Carbon Dioxide and Climate Impulse Response Functions for the Computation of Greenhouse Gas Metrics: A Multi-Model Analysis. *Atmospheric Chemistry and Physics* 13 (5):2793–2825.

Kelly, David L and Charles D Kolstad. 1999. Bayesian learning, growth, and pollution. *Journal of Economic Dynamics and Control* 23 (4):491–518.

Klibanoff, Peter, Massimo Marinacci, and Sujoy Mukerji. 2005. A smooth model of decision making under ambiguity. *Econometrica* 73 (6):1849–1892.

Kogan, Leonid, Dimitris Papanikolaou, Amit Seru, and Noah Stoffman. 2017. Technological innovation, resource allocation, and growth. *The Quarterly Journal of Economics* 132 (2):665–712.

Kogan, Leonid, Dimitris Papanikolaou, and Noah Stoffman. 2020. Left behind: Creative destruction, inequality, and the stock market. *Journal of Political Economy* 128 (3):855–906.

Kreps, David M. and Evan L. Porteus. 1978. Temporal Resolution of Uncertainty and Dynamic Choice. *Econometrica* 46 (1):185–200.

Lemoine, Derek and Christian P Traeger. 2016. Ambiguous tipping points. *Journal of Economic Behavior & Organization* 132:5–18.

Levitan, David. 2013. Quick-Change Planet: Do Global Climate Tipping Points Exist? *Scientific American* .

Li, Xin, Borghan Narajabad, and Ted Temzelides. 2016. Robust dynamic energy use and climate change. *Quantitative Economics* 7 (3):821–857.

Lucas Jr, Robert E and Edward C Prescott. 1971. Investment under uncertainty. *Econometrica: Journal of the Econometric Society* 659–681.

Maenhout, P J. 2004. Robust Portfolio Rules and Asset Pricing. *Review of Financial Studies* 17:951–983.

Nordhaus, William D. 2017. Revisiting the social cost of carbon. *Proceedings of the National Academy of Sciences* 114 (7):1518–1523.

Novy-Marx, Robert. 2007. An equilibrium model of investment under uncertainty. *The review of financial studies* 20 (5):1461–1502.

Ricke, Katharine L. and Ken Caldeira. 2014. Maximum Warming Occurs about One Decade After a Carbon Dioxide Emission. *Environmental Research Letters* 9 (12):1–8.

Rising, James, Marco Tedesco, Franziska Piontek, and David A Stainforth. 2022. The missing risks of climate change. *Nature* 610:643–651.

Rudik, Ivan. 2020. Optimal Climate Policy When Damages Are Unknown. *American Economic Journal: Economic Policy* 12 (2):340–73.

Stalard, Esme. 2024. Nuclear Fusion: New Record Brings Dream of Clean Energy Closer. *BBC, February 8* .

Stine, Deborah D. 2008. The Manhattan Project, the Apollo program, and federal energy technology R & D programs: A comparative analysis. Tech. rep., Congressional Research Service, the Library of Congress.

Weitzman, Martin L. 2009. On modeling and interpreting the economics of catastrophic climate change. *The Review of Economics and Statistics* 91 (1):1–19.